DTIC

Construction, Characterization and Evaluation of the AMRL Flyer Sensitivity Test Apparatus

David J. Hatt and
Michael G. Wolfson

DTIC

DEPARTMENT OF DEFENCE
DEFENCE SCIENCE AND TECHNOLOGY ORGANISATION

Construction, Characterization and Evaluation of the AMRL Flyer Sensitivity Test Apparatus

David J. Hatt and Michael G. Wolfson

Weapons Systems Division
Aeronautical and Maritime Research Laboratory

DSTO-TR-0218

ABSTRACT

The AMRL flyer sensitivity test apparatus (FSTA) uses the electric gun technique to accelerate 50 μm thick plastic flyer plates of about 3.5 mm in diameter to high velocity. Impacting high explosives with the flyer plates generates short duration shock pulses with sufficient energy to cause ignition. By varying the charge voltage, and hence the flyer velocity, the relative shock sensitivity of explosives can be measured. Detonation or non-detonation of the explosive is indicated by the level of damage to a steel witness plate. The FSTA was found to be suitable for testing 50 mg samples of pressed explosives with shock sensitivities in the range represented by PETN (high) to Composition B (low). A flyer velocity versus charge voltage calibration up to a charge voltage of 6 kV was performed using a VISAR velocity interferometer. The shock sensitivity can be related to charge voltage in the range 5-10 kV or flyer velocity in the range 2-4 km/s. A comparison of the FSTA with similar USA testers is presented.

DEPARTMENT OF DEFENCE

DEFENCE SCIENCE AND TECHNOLOGY ORGANISATION

Published by

DSTO Aeronautical and Maritime Research Laboratory
PO Box 4331
Melbourne Victoria 3001

Telephone: (03) 626 8111
Fax: (03) 626 8999

AR No. 009-347
January 1996

APPROVED FOR PUBLIC RELEASE

Construction, Characterization and Evaluation of the AMRL Flyer Sensitivity Test Apparatus

Executive Summary

Shock sensitivity testing of military explosives is one of many tests that must be performed to indicate the suitability of these explosives for their intended end use. It is one of a number of tests that have been employed over many years by WSD-AMRL (Maribyrnong) in order to provide expert advice on explosive performance, safety, and service life issues to the Australian Defence Force (ADF). An important parameter that can affect the shock sensitivity is the particle size of the explosive constituents. Moreover, with advances in the technology currently being used or likely to be used in the near future for the ignition of explosives, particle size effects increasingly need to be considered with respect to the duration of the shock pulse (i.e., substained versus short durations). Nearly a decade ago, a program of work was commenced at WSD to study particle size effects on the shock sensitivity of explosives. The first phase of this work employed sustained shocks produced by the WSD small-scale gap test which, in effect, uses a small explosive pellet to produce the shock pulse. For many years this was the only shock sensitivity testing method available at WSD. Further phases awaited the development of test equipment based on the electric gun technique of propelling small, thin plastic flyer plates to high velocity which are in turn used to impact the explosive under test to produce the short duration shock pulses.

A number of USA defence establishments make flyer plate shock sensitivity tests with equipment based on that developed by USA workers,Voreck and Velicky. It seemed desirable that the AMRL flyer sensitivity test apparatus (FSTA) should replicate the USA arrangement as closely as possible to facilitate comparison of data, particularly sensitivity data. Thus, the AMRL FSTA was constructed using similar components and has a similar system layout.

Following construction, calibration of the FSTA was attempted using a VISAR velocity interferometer system. Calibration yields the relationship between the electric gun's capacitor charge voltage and flyer plate velocity. Sensitivity tests for TNT, Composition B, RDX, and PETN were then performed. All of these explosives are commonly used in munitions in the ADF inventory. The tests for TNT and PETN were to be representative of the low and high sensitivity range of the FSTA, respectively. Both the calibration and the explosive tests revealed a significant difference in performance for the AMRL FSTA and the USA equipment. The difference in performance is attributed to the different electrical circuit parameters. While detonation of TNT could not be achieved employing the FSTA, it is expected that the FSTA will be suitable for extending the particle size effect studies as required for explosives with shock sensitivities within its shock sensitivity range (e.g., for explosives at least as shock sensitive as RDX). This capability should be sufficient to enable WSD to meet the currently perceived level of support for the ADF. Modification of the FSTA to enable testing on less shock sensitive explosives (e.g., TNT) could be undertaken in the future if required.

Authors

David J. Hatt
Weapons Systems Division

David Hatt graduated Dip App Physics from the Ballarat School of Mines and Industries in 1968, and joined AMRL in 1969. Until transferring to the Explosives Ordnance Division (now Weapons Systems Division) in 1977, he worked on Defence standards and calibration systems. He has specialized in the development and application of instrumentation for the study of high-speed events and phenomena related to explosives and ammunition.

Michael G. Wolfson
Weapons Systems Division

Mike Wolfson has gained extensive experience in over thirty years working exclusively in the explosives R&D field in both England and Australia. He joined AMRL in 1964, working initially on explosives formulation, and device development and testing, and later on the measurement of detonation parameters. He is a specialist in the application of electronic and photoinstrumentation techniques for determining the performance and effects of explosives and munitions. His publications cover a diverse range of topics from explosives polishing techniques to ship shock testing.

Contents

1. Introduction

As reported previously [1], a program of work was commenced at AMRL to study particle size effects on the shock sensitivity of explosives using both sustained and short duration shocks. The first phase of this work employed sustained shocks produced by the AMRL small-scale gap test (SSGT) [2]. Further phases awaited the development of test equipment based on the electric gun technique of producing flyer plates [3].

A number of USA defence establishments perform flyer plate shock sensitivity tests with equipment based on that developed by Voreck and Velicky [4]. At the time of development of the equipment, their particular interest was in measurements for evaluating the sensitivity of booster explosives to shock pulses similar to those produced by detonators. It was reported that the flyer tests more closely approximated the initiation of booster explosives in fuzes by fragments from a detonator than the Naval Ordnance Laboratory SSGT. In addition, the flyer test can be used to predict critical energy. Velicky [5] has also used the test to investigate factors responsible for in-bore thermal explosions associated with Composition B.

It seemed desirable that if possible the AMRL flyer sensitivity test apparatus (FSTA) should replicate the USA arrangement to facilitate comparison of data, particularly sensitivity data. Thus, the AMRL FSTA was constructed using similar components and has a similar system layout. It employs a 16 μF/20 kV energy storage capacitor and has circuit inductance and resistance values of 180 nH and 0.050 ohm, respectively. Typical specifications for the USA equipment are capacitance of 14.5 μF, inductance of 140 nH, and resistance of 0.025 ohm [4,6]. The Mylar flyer plates used in both systems have nominally the same thickness of 50 μm. However, the aluminium bridge foil thickness used in the USA system is 25 μm compared to 35 μm used in the AMRL system.

Following construction, calibration of the FSTA was attempted using a VISAR velocity interferometer [7]. Calibration yields the relationship between capacitor charge voltage and flyer plate velocity. Due to electromagnetic noise (EMI) problems, only a partial calibration was achieved. Sensitivity tests for TNT, Composition B, RDX, and PETN were then performed. The tests for TNT and PETN were to be representative of the low and high sensitivity range of the FSTA, respectively. Both the calibration and the explosive tests revealed a significant difference in performance for the AMRL FSTA and the USA equipment; as a consequence, data for TNT could not be obtained. The difference in performance is attributed to the different electrical circuit parameters. However, it is expected that the FSTA will be suitable for extending the particle size effect studies for explosives with shock sensitivities within its shock sensitivity range (e.g., for explosives at least as shock sensitive as RDX).

The present report includes a decription of mechanical and electrical details of the AMRL FSTA, procedures used for calibration and sensitivity testing, and test data.

2. Design and Construction

2.1 Mechanical

Schematic diagrams of the FSTA are shown in Figures 1 and 2. The frame (51 mm x 51 mm x 3 mm mild steel angle) is covered on the top, front, and sides by 0.91 mm thick steel panels. The rear is covered by a perforated steel panel which provides ventilation for the dump resistors. Initially, the FSTA had no bottom panel but subsequently one was added to enhance the screening of electromagnetic radiation when the system is fired (see Section 3 below). The overall dimensions of the FSTA are 1.2 m (wide) x 0.7 m (deep) x 1.12 m (high) [8].

An explosives test cell is located at the front top left of the FSTA. The test cell has a 6 mm thick steel sliding cover which is opened when required to install the test sample. The sliding cover is mounted on a 12.5 mm thick steel base plate and in the closed position fits against a 6 mm thick steel angle plate. The bus bars from the capacitor protrude into the test cell via an opening in the base plate. Copper electrodes are attached to the end of the bus bars. The explosive sample assembly is clamped against the electrodes by means of a copper clamp bar.

2.2 Electrical

The HV capacitor (CSI Technologies Inc., Model No. 20N7318/LNP) has the following specifications (CSI catalogue): capacitance of 16 μF, maximum charge voltage of 20 kV, peak discharge current of 100 kA, and an inductance of 40 nH. The capacitance values measured using a capacitance bridge (GenRad RLC Digibridge, Model 1657) were 16.3 μF at a test frequency of 1 kHz and 16.4 μF at 100 Hz. The inductance and resistance values measured at a charge voltage of 5 kV using the arrangement shown in Figure 3 were 115 nH and 0.04 ohm, respectively. This arrangement was devised in an attempt to minimize external inductance and resistance effects. Discharge of the capacitor was activated by removing a strip of Mylar by hand from between the gap in the copper bars. The current-time history of the discharge was measured using a Rogowski coil [9] and a passive integrator [10]. The inductance and resistance were calculated using the ringdown equations [4]. When installed in the system, the capacitor is connected to the bus bars, unavoidably adding inductance and resistance to the circuit. In an attempt to minimize these increases, the bus bars are made from 3 mm (thick) x 25 mm (wide) copper and clamped closely together where possible. Where the bus bars are less than 30 mm apart, they are wrapped in Mylar foil insulation. From discharges performed at 5 kV with the bus bars shorted via a shorting link clamped against the electrodes, the circuit inductance and resistance were found to be 180 nH and 0.050 ohm, respectively. The shorting link had the same dimensions as the copper striplines used in explosives tests. During these measurements, the current-time history was measured using the system's current transformer (Pearson

Electronics, Model 301X). The output of the current transformer in turn was measured using a 100 MΩ 1000:1 75 MHz HV probe (Tektronix, Model P6015) . The transformer and probe were interconnected by 15 cm of URM67 coaxial cable. Discharge of the capacitor was activated by electromechanically removing a Kapton insulator (comprising two 50 μm thick Kapton sheets held together by double-sided adhesive tape) from between the electrodes.

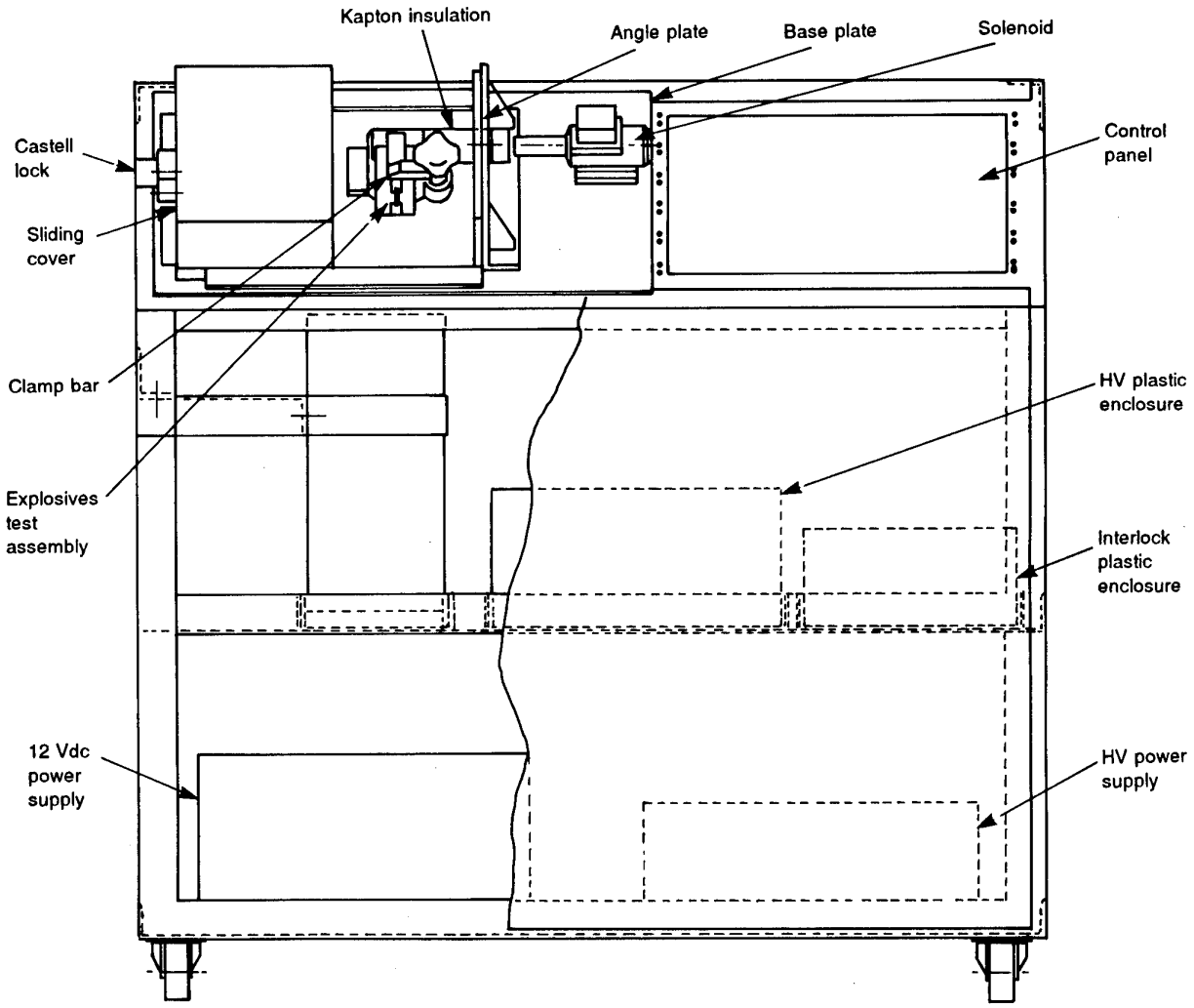

Figure 1: *The AMRL Flyer Sensitivity Test Apparatus - front view.*

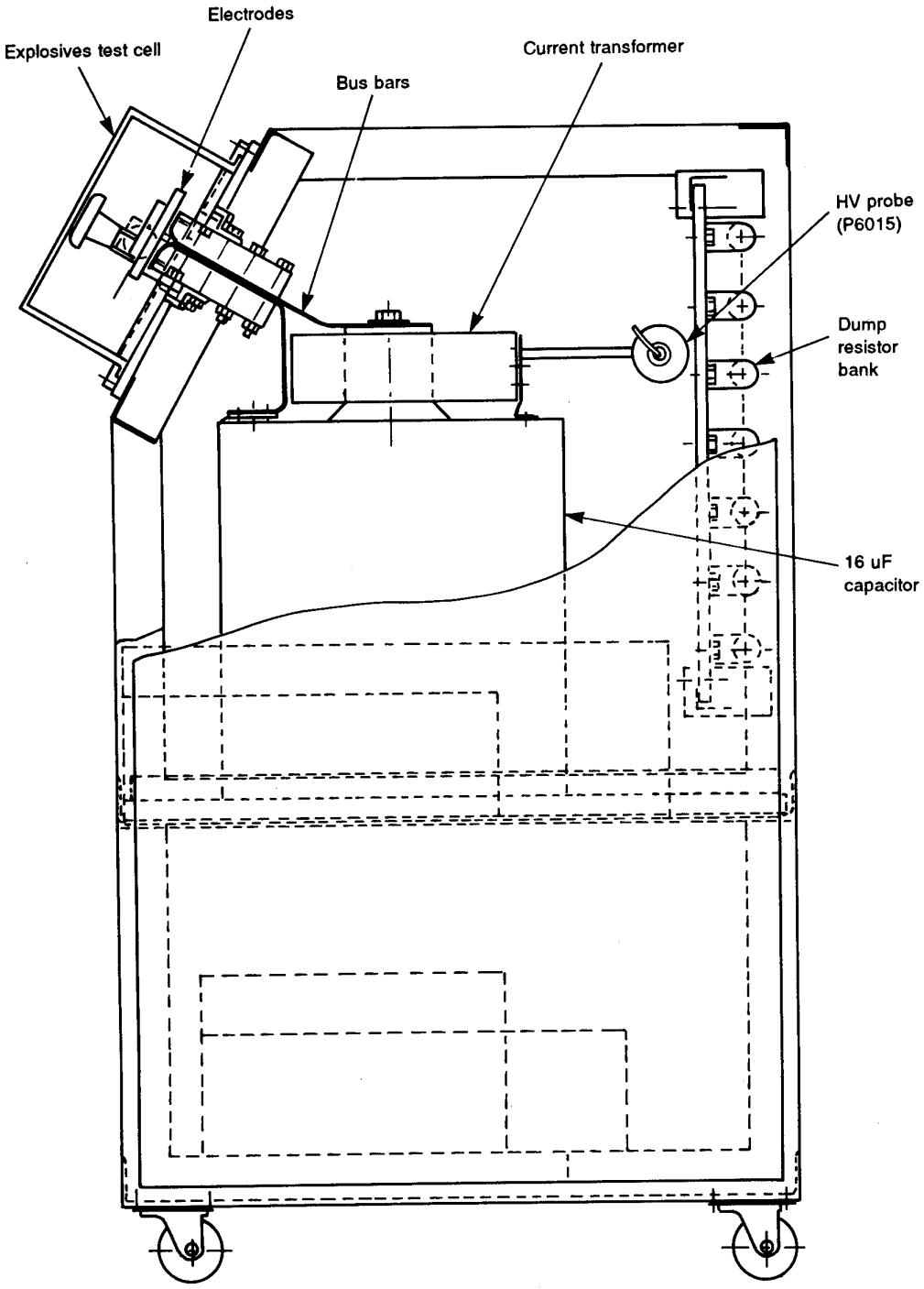

Figure 2: The AMRL Flyer Sensitivity Test Apparatus - side view.

The electrical circuit (Fig.4) interconnecting the capacitor and the 20 kV/10 mA HV power supply (Hartley Measurements Limited, Model 421) comprises a 10 kΩ/1600 W dump resistor bank, 25 kV relays (Kilovac, Model H-17), 15 kV overvoltage spark gap (EG&G, Type OGP-44G-15) and a 1 GΩ 1000:1 HV dc-probe (Radio Spares). To protect the spark gap from repetitive conduction in the event of an overvoltage condition, a transistor-driven relay is used to shut down the HV power supply via its panel interlock. The HV relays, spark gap, and HV dc-probe are housed in the HV plastic enclosure (Fig.1).

Charge and *Isolate* push-button switches on the control panel (Fig.1) are used to enable the connection of power to the HV relays. A *Fire* push-button enables the connection of the 12 Vdc/10 A power supply to a solenoid that electromechanically retracts a bolt connected to the Kapton insulation between the electrodes. The panel is also fitted with a multiturn potentiometer and push-button switch for remote control of the HV power supply, and a key-release latching *Dump* switch for emergency shut-down of the FSTA. Primary control of power to the FSTA is via a castell-key switch, which is also located on the control panel. In addition, the HV relays or power supplies cannot be operated if any of the interlock switches on the FSTA panels are open. The interlock relays and related power sources are housed in the Interlock plastic enclosure (Fig.1).

2.3 System Safety

To achieve electrical and explosives safety, a mechanical castell lock on the sliding test cell cover and the electrical castell-key switch share an unique key, and are used to interlock the sliding cover with the electrical circuits. The cover can only be opened by using the key which becomes captive in the lock while the cover is open; thus the castell-key switch is off and the FSTA is held in the fail-safe configuration (capacitor isolated from the power supply and connected to dump resistors). Conversely, the cover must be locked before the key can be retrieved and used to activate the electrical circuits via the key switch. When the key is in the possession of the operator, explosive and electrical safety are assured.

3. Calibration

Sensitivity data based on electric gun flyer tests are often given simply in terms of the capacitor charge voltage. This is analogous to the approach used over many years in the AMRL SSGT where data is reported in terms of a gap (barrier) thickness [2]. However, it is much more useful to have data based on the flyer velocity; this then enables the pressure-time history of the shock pulse into the explosive to be defined.

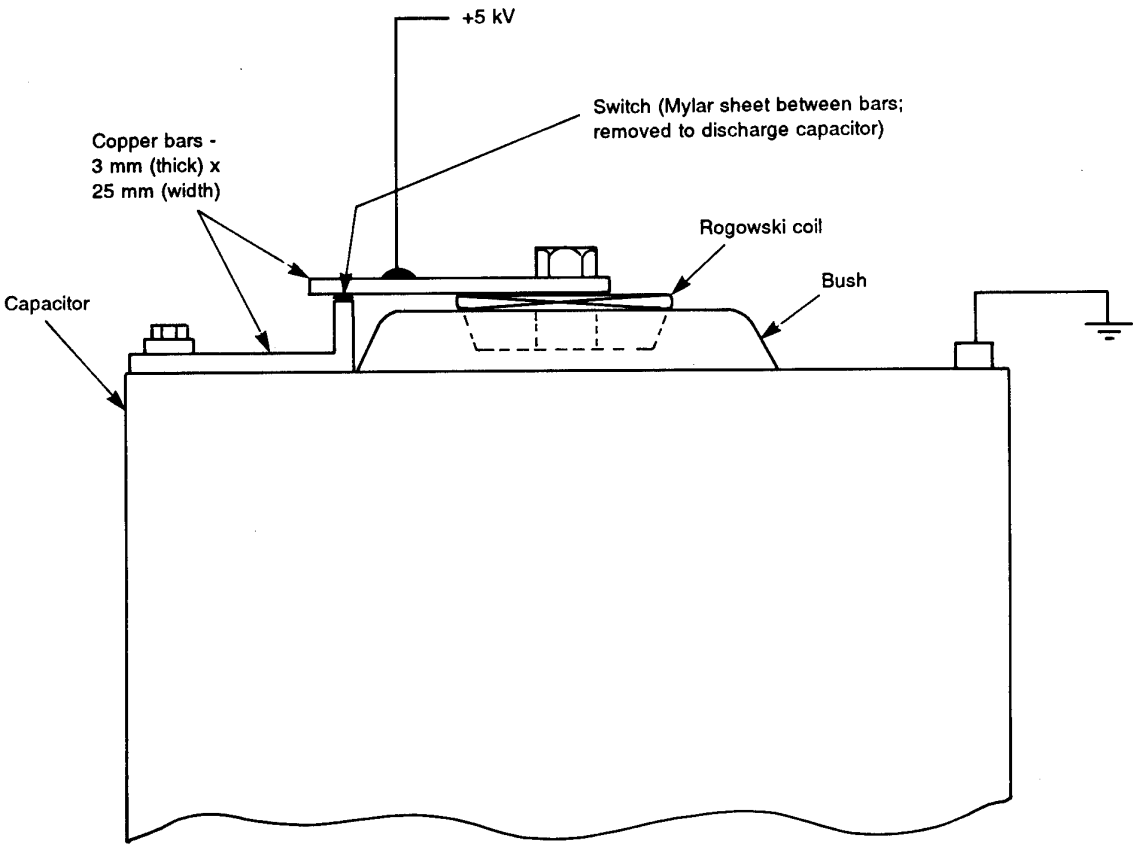

Figure 3: Schematic diagram of the arrangement employed for the measurement of capacitor inductance and resistance.

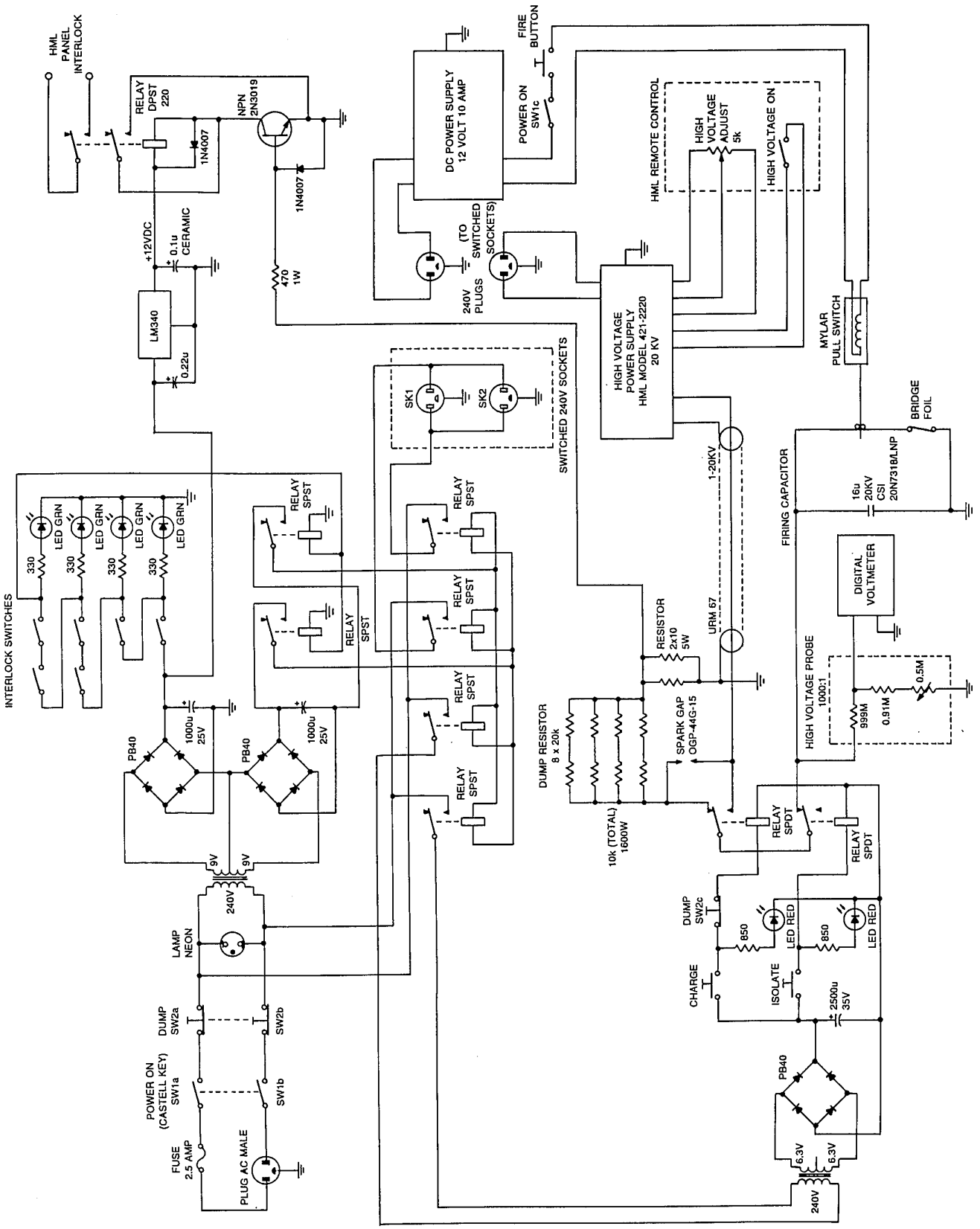

Figure 4: Circuit diagram of the AMRL Flyer Sensitivity Test Apparatus.

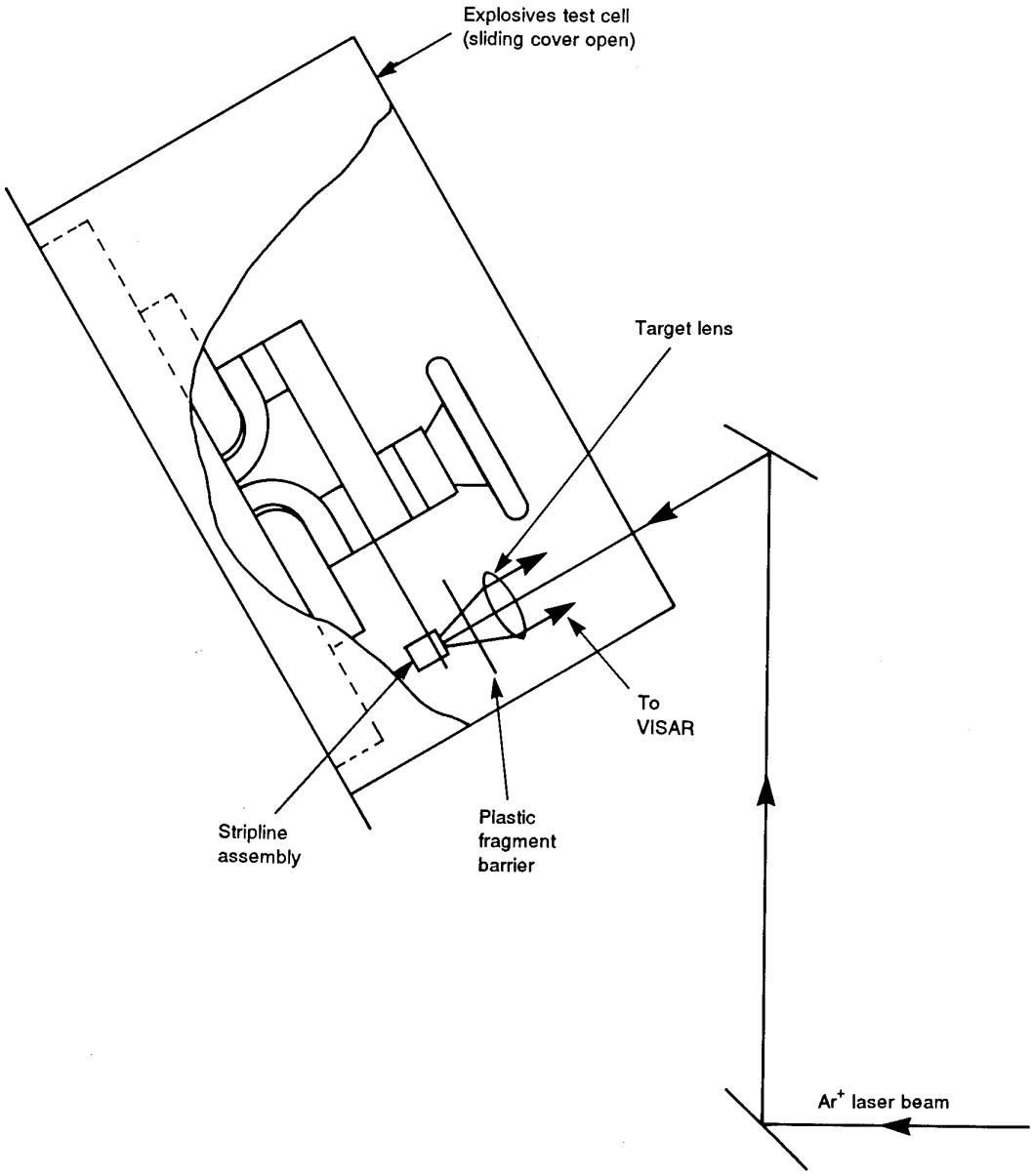

Figure 5: Schematic diagram of the optical arrangement employed for focusing of the laser beam onto the flyer target and for return of the diffusely reflected beam to the VISAR.

The performance of the system is directly evaluated, thereby avoiding difficulties introduced by an evaluation based on the response of an explosive to the particular FSTA configuration used. Should a change in performance of the FSTA be suspected, a diagnosis is easily effected by flyer velocity measurement. Flyer velocity after travelling the length of the barrel (i.e., on impact with the explosive), rather than the peak velocity, is required for the calibration.

For the calibration, the explosives test cell sliding cover needed to be in the open position to enable the VISAR laser beam to impinge on the flyer (Fig.5). Consequently, to facilitate safety of operations, the calibration was performed with the FSTA in an earthed screened room [11] where the FSTA was configured for remote control of the charging/discharging of the capacitor. A HV power supply located outside the screened room was used instead of the FSTA's integral HV power supply for charging the capacitor. A safety interlock system [11] controlled, in turn, power to the HV power supply, charging of the capacitor, and isolation of the charged capacitor from the supply. A remote *Fire* push-button enabled the connection of the 12 Vdc power to the solenoid via an electromechanical relay. All of these controls were held in a disabled state by the safety interlock system when room doors were open. In addition to providing a limited access work area, the screened room reduced electromagnetic interference effects on external instrumentation and, as the FSTA was located in an explosives building, reduced the RF hazard for some types of electro-explosive devices that could be in the building.

The VISAR laser beam entered the screened room through metallic waveguides [11]. The flyer surface was grit blasted for diffuse reflection and an electro-optic shutter limited the time the flyer was exposed to high laser beam power (range 0.5 - 0.7 W) [12]. The stripline assemblies were prepared as detailed in Appendix A but excluded the explosives sample holder and witness disc.

The VISAR photomultiplier tubes (PMTs) operate in pulse mode and need to be triggered < 1 ms before flyer motion. For most shots, synchronization was achieved by using a capacitor discharge circuit which was discharged when a pair of brass pins were shorted on contact with a metal arm. Before firing, a small gap separated the arm and pins. During firing, the gap was closed when one end of the arm was lifted by a nylon disc attached to the solenoid bolt. This method of triggering tended to be unreliable and, therefore, for some shots the PMTs were triggered by a pulse from an optoelectronic circuit. A photodetector in this circuit was coupled to one end of a fibre optic cable, the other end of which was set up in close proximity to the upper FSTA electrode to collect broadband radiation from the discharge arc. The VISAR signals were recorded by a digital storage oscilloscope (DSO) which was triggered by a second optoelectronic circuit, again with a fibre optic cable collecting the arc radiation.

In addition to the relationship between flyer velocity and charge voltage, a number of other relationships were investigated during the calibration. These relationships are shown in Table 1. Burst specific action, g_o, is defined [13,14] by

$$g_o = \int_o^{t_b} J^2(t)dt \qquad (1)$$

where J = current density in the bridge foil.

As mentioned above, the circuit current-time history is normally measured by means of a current transformer and a HV probe. During calibration, the DSO for recording the current, i, was located close to but outside the screened room. At this position, the DSO was out of range of the standard HV probe cable. In an alternative arrangement (Fig. 6), the HV probe was replaced with a another current transformer (Tektronix, Model CT-2). However, it was necessary to use a HV probe for the measurement of the bridge foil voltage, V_{bf}, shown in Figure 7. This required the addition of 1 m of cable between the probe compensating box and the DSO. Tests using a square wave signal from a function generator showed that the probe's bandwidth was little changed by the added cable while the attenuation ratio changed to 1210:1. The probe voltage, V_p, was also corrected for an induced voltage component [10,12]; thus

$$V_{bf}(t) = V_p(t) - L_p di/dt \qquad (2)$$

and the inductance, L_p, was calculated from

$$L_p = V_i(t)/(di/dt) = 32 \quad \text{nH} \qquad (3)$$

where V_i = the induced voltage signal during a ringdown and *di/dt* was obtained from the corresponding current signal. A first estimate of L_p was made using the initial voltage step on the induced voltage signal. This was tested for the complete voltage signal and adjusted for repeat tests to find a value that gave the best overall result (i.e., until the corrected signal least deviated from zero). Strictly speaking, V_{bf} includes the voltage across a portion of the bus bar but this is negligibly small.

Table 1: *List of relationships investigated during calibration.*

Nomenclature	V_c	Charge voltage	
	u_f	Flyer velocity	
	I_m	Peak current	
	P_m	Peak power	
	V_b	Burst voltage	
	I_b	Burst current	
	t_b	Time-to-burst	
	E_b	Energy-deposited-up-to-burst	
	g_o	Burst specific action	
	J_b	Burst current density	
Relationships	u_f	vs	V_c
	I_m	vs	V_c
	P_m	vs	V_c
	V_b	vs	V_c
	I_b	vs	V_c
	t_b	vs	V_c
	E_b	vs	V_c
	u_f	vs	E_b
	u_f	vs	J_b

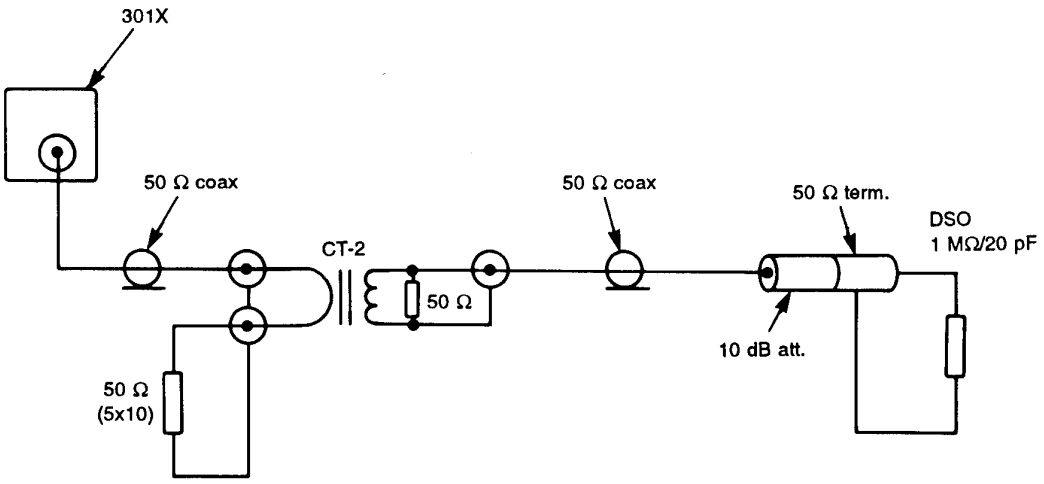

Figure 6: *Schematic diagram of the arrangement employed for the measurement of the circuit current. Coupling to the stripline is via the 301X current transformer as shown in Figures 1 and 2.*

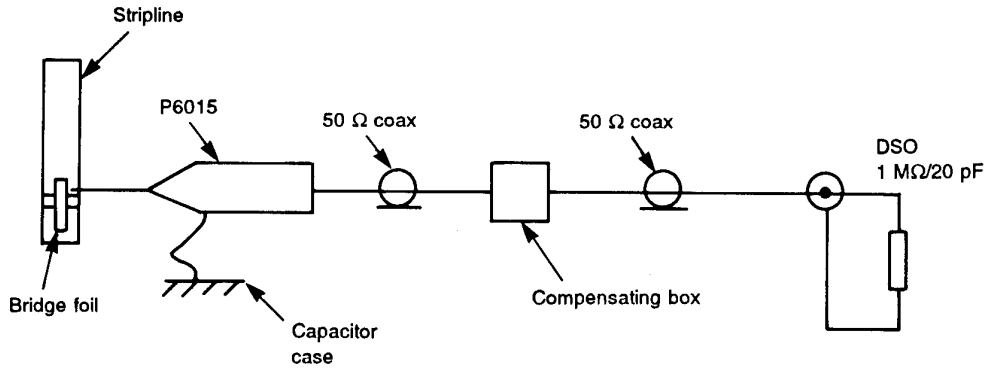

Figure 7: Schematic diagram of the arrangement employed for the measurement of the bridge foil voltage.

The voltage and current signals stored by the DSO were transferred via a GPIB (IEEE-488) communications channel to a personal computer. Data reduction was performed by means of Asystant GPIB [15] routines. Initially a problem occurred with the probe voltage correction due to high frequency electromagnetic noise on the current signal over about the first eighth cycle of the signal. Though the noise amplitude was fairly small, it became significant on differentiation. The noise amplitude on the corrected signal was greatly reduced by using a smoothed version of the current signal. The bridge foil electrical power was derived from the product $V_{bf}\,i$ while energy was determined by the time-integration of this product. The burst current and energy-deposited-up-to-burst values were taken as those corresponding in time to the burst voltage (the peak in the bridge foil voltage signal).

4. Explosives Tests

The series of explosive sensitivity tests used the Bruceton method [16] and began with PETN (plus 0.2% cetyl alcohol) pressed to a density of 1.6 Mg/m^3, corresponding to a theoretical maximum density (TMD) of 90%. The Bruceton test interval was 200 volts. The stripline and explosive test assemblies were prepared as described in Appendix A. Prior to each shot, the stripline outer faces and the bus bar electrodes were visually inspected to assess (subjectively) the amount of surface contamination present.

Generally, after each fifth firing, they were cleaned by lightly rubbing with wet/dry silicon carbide paper followed by wiping with a tissue wetted with ethanol.

A detonation was considered to have occurred when a clean hole was punched in the witness disc. For PETN, deciding whether the event was a detonation or a non-detonation was fairly straight forward. But, as will be shown later, discriminating between the two is not always so clear cut.

TNT was tested at a density of 1.49 Mg/m^3 (90% TMD). Four shots were performed starting at a charge voltage of 8 kV and ceasing at 14 kV without attaining a detonation. There was essentially no denting of the witness disc at 8 kV and 10 kV, mild denting at 12 kV, and significant denting at 14 kV.

Tests for Composition B at a density of 1.44 Mg/m^3 (83% TMD) also failed to produce a detonation. The samples were prepared by pressing particulate Composition B obtained by grinding cast Composition B (60%RDX/40%TNT/1% wax). Three shots performed at voltages in the range 10-12 kV produced only mild denting of the witness discs.

Successful tests for Composition B (60%RDX/40%TNT/no wax) were obtained at a density of 1.59 Mg/m^3 (92% TMD). The samples were prepared by pressing material from a batch of manually-mixed ground TNT and RDX Grade A, Class 1 (recrystallised). At the commencement of these tests some difficulty was experienced in establishing the Bruceton go/no-go pattern. Resistance measurements suggested that this seemed to be related to high stripline resistance. The stripline assemblies were ones that had been prepared a little over two weeks prior to testing. For some shots using these assemblies the peak current was lower than expected and the time-to-peak was longer than expected. The static resistance across the gap in the stripline was found to be several ohms compared to about 0.025 ohms for a freshly laid bridge foil. Subsequent shots used only freshly laid bridge foils. For some of these shots, the discrimination between detonation and non-detonation was poorly defined because the denting of the witness disc was severe enough to produce a small crack. For these cases, the sample holders were also examined for the lateral expansion which occurs for a detonation; if expansion was not evident, the event was recorded as a non-detonation.

Before the Bruceton run for this Composition B could be completed it was stopped in order to replace the Mylar wrapping around the bus bars. Cumlative damage to the exposed end of the wrapping near the positive electrode from the discharge arc had eventually caused self-firing of the circuit at high charge voltage. In an attempt to prevent arc damage to the refurbished bus bars, glass cloth insulation tape was wrapped around the exposed Mylar wrapping. After reassembly, ringdown tests were performed and showed that the system inductance and resistance were unchanged. The Bruceton test was completed but the post repair data seemed to show an upward trend for the firing voltage.

A repeat Bruceton test was performed for PETN to investigate the possibility that the FSTA had changed in some way. In fact the results were in good agreement with those previously obtained for PETN indicating no change to the FSTA had occurred. The opportunity was taken during these tests to determine the testing rate; this was found to be about 12 shots/hr using completed stripline assemblies.

The last explosive to be tested was RDX Grade A, Class 1 (recrystallised) at a density of 1.65 Mg/m^3 (92% TMD). Detonations were obtained, as might be expected based on its known relative shock sensitivity to PETN and Composition B.

5. Results and Discussion

5.1 Calibration

The flyer velocity-time histories were integrated to obtain distance-time histories. These two sets of data enabled velocity-distance histories to be formed from which the flyer velocities at a distance of 0.8 mm (barrel length) were extracted. An example velocity-distance history is shown in Figure 8. The calibration data are shown in Table 2, and in Figure 9 as a plot of flyer velocity versus charge voltage. The range for V_c was 4.6-6.0 kV. The low end of this range is considered to be a little above the charge voltage corresponding to the onset of flyer formation. Velocity data above 6 kV were required but this could not be attained due to high levels of EMI on the VISAR PMT signals. For the calibration, the PMT units were about 2 m away from the FSTA. Post calibration tests with the PMT units removed from the VISAR and located further away in an adjoining room showed that the noise levels would be significantly reduced with the VISAR in this location. For any future attempt at extending the calibration above 6 kV, a fibre-optic conversion of the VISAR is proposed to facilitate its relocation to this room.

***Table 2:** Flyer velocity and charge voltage data.*

V_c (kV) (kV)	VISAR fringe constant (m/s)	u_f (@ 0.8 mm) (m/s)
4.60	901	900
4.61	901	600
5.26	901	1600
5.38	901	1800
4.69	1698	750
5.02	1698	1050
5.29	1698	1450
5.29	1698	1600
5.46	1698	1800
5.55	1698	2150
5.61	1698	1650
5.76	1698	1850
5.99	1698	2000

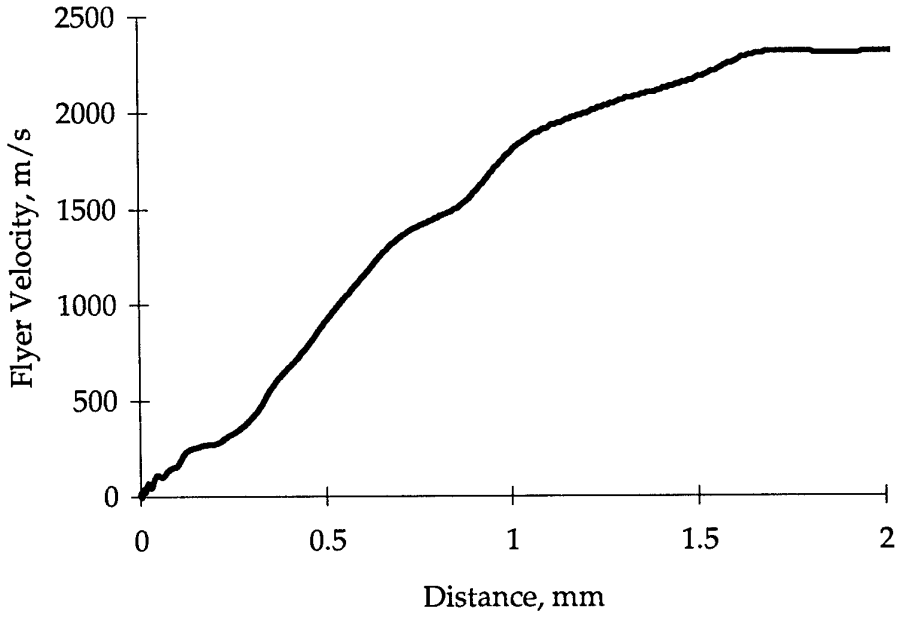

Figure 8: Velocity-distance history at a charge voltage of 5.29 kV.

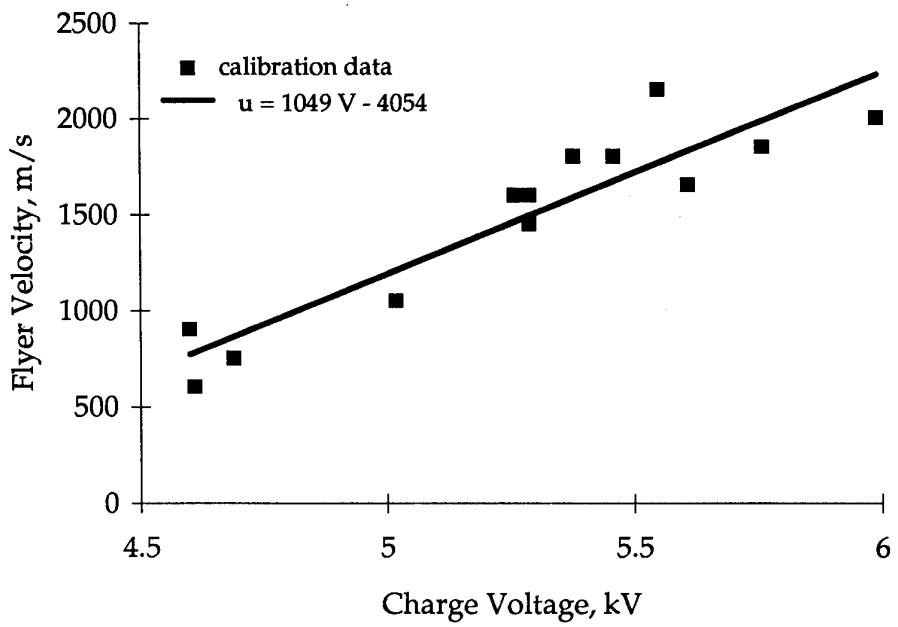

Figure 9: Flyer velocity (at 0.8 mm) versus charge voltage calibration curve.

A model commonly used for predicting the terminal velocity of electrically-driven flyer plates is the electrical Gurney equation; for massive tamping, the terminal velocity, u, is given by the following expression [17]:

$$u = \sqrt{2E_g}(M/C + 1/3)^{-1/2} \quad (4)$$

where E_g = the electrical Gurney energy;
M = flyer plate mass per unit area; and
C = bridge foil mass per unit area.

Further,

$$E_g = KJ_b{}^n \quad (5)$$

where J_b = the burst current density and K and n are experimentally determined constants.

The model is not strictly applicable to the FSTA calibration data as the flyer plate at 0.8 mm has not quite reached terminal velocity. Nevertheless, the velocity and current density data were fitted using the same functional form, viz.

$$u_f{}^2(M/C + 1/3)/2 = K' J_b{}^{n'} \quad (6)$$

where the primes are used to indicate that the values are derived from non-terminal velocity data. Thus for the Mylar flyer plate of 52 μm thickness and aluminium bridge foil of 34 μm thickness, flyer plate velocity in km/s and current density in GA/m^2, the values for K' and n' were found to be 1.54×10^{-4} and 1.91, respectively.

Typical current, bridge foil voltage, power, energy, and specific action-time histories are shown in Figures 10,11,12,13, and 14, respectively, for a charge voltage of 5.29 kV. The calibration data for flyer velocity and burst current density are shown plotted in Figure 15 along with the calculated curve using equation 6. The curve is presented over a greater burst current density range than that for the calibration data since the experimental data for the various electrical parameters were obtained over a greater charge voltage range, viz. 4.6-10.0 kV (Table 3). For comparison, a curve for the predicted terminal velocity is also shown using $K = 1.657 \times 10^{-3}$ and $n = 1.526$ [17] in equation 5.

Scatter diagrams for charge voltage vs peak current, burst current, burst voltage, peak power, energy-up-to-burst, time-to-burst, and burst current density are shown in Figures 16,17,18,19,20, 21, and 22, respectively. These plots provide a comprehensive characterization the FSTA system.

Table 3: *Measured and calculated values for peak and burst current, burst voltage, peak power, energy-up-to-burst, time-to-burst, specific action, and burst current density.*

V_c (kV)	I_m (kA)	I_b (kA)	V_b (kV)	P_m (MW)	E_b (J)	t_b (μs)	$g_o \times 10^{16}$ (A^2s/m^4)	J_b (GA/m²)
4.97	34.8	22.9	1.381	31.6	34.9	3.76		
4.97	34.8	19.0	1.234	23.4	33.9	4.04		
5.03	33.8	14.4	1.057	15.2	30.0	4.42		
5.05	36.0	21.0	1.545	32.4	34.2	3.80		
5.00	34.8	20.5	1.394	28.6	43.3	4.04	6.52	91.4
5.04	36.3	23.7	1.815	43.0	33.2	3.62		
5.02	34.8	20.5	1.679	34.4	36.8	3.88	5.99	90.7
4.99	34.8	24.5	1.766	43.3	43.8	3.68	6.58	112.9
5.00	34.8	20.5	1.815	37.2	37.3	3.82	5.60	91.6
5.00	34.0	20.5	1.396	28.6	33.0	3.74	5.50	92.8
5.06	36.3	26.1	1.773	46.3	43.3	3.48	6.01	120.9
4.60	31.6	9.5	0.970	9.2	27.8	4.42	4.76	43.3
5.40	37.1	31.6	1.721	54.4	39.7	3.28	6.17	145.2
5.44	37.1	30.0	1.744	52.3	39.1	3.26	5.71	136.8
4.61	31.6	9.5	0.602	5.7	25.2	4.58	4.94	42.7
5.38	37.1	26.1	2.117	55.3	42.7	3.48	5.81	118.1
5.50	36.3	30.8	1.999	61.6	38.3	3.26	5.78	140.9
5.29	36.3	27.6	2.186	60.3	46.0	3.50	6.00	123.9
5.22	37.1	26.9	2.228	59.9	43.7	3.44	5.79	120.2
5.26	36.0	27.2	1.854	50.4	41.6	3.44	5.93	121.2
5.29	37.6	28.3	1.922	54.4	39.3	3.40	5.74	126.1
5.29	36.0	25.0	1.861	46.5	40.9	3.58	5.53	112.3
5.29	36.8	25.8	2.149	55.4	35.2	3.54	5.73	115.9
5.28	36.0	26.5	1.990	52.7	40.2	3.44	5.99	118.5
5.65	39.8	33.2	2.469	82.0	35.0	3.04	6.06	149.1
5.02	33.8	23.9	1.112	26.6	35.1	3.76	6.32	106.5
5.30	36.3	30.0	1.961	58.8	39.5	3.32	5.87	133.7
5.27	33.8	18.8	1.464	27.5	30.9	4.02	5.60	83.4
5.55	38.2	32.1	2.452	78.7	28.7	3.02	5.85	145.7
5.56	37.1	31.0	2.102	65.2	38.1	3.20	5.78	139.6
5.61	38.7	30.0	2.332	70.0	35.3	3.26		
5.46	37.1	28.8	2.292	66.0	35.2	3.24	5.60	130.7
5.99	40.4	34.9	2.483	86.7	37.8	2.98	6.03	159.1
6.00	41.6	37.1	2.243	83.2	37.4	2.88	6.26	169.7
6.27	43.8	39.3	2.273	89.3	39.5	2.74	6.07	177.0
6.30	43.8	38.7	2.702	104.6	41.0	2.72	6.14	175.1
6.28	41.1	37.9	2.200	83.4	35.6	2.88	6.35	173.4
6.22	40.4	36.5	2.553	93.2	35.9	2.86	5.88	166.4
6.22	40.9	37.1	2.613	96.9	37.6	2.88	5.43	167.1
6.20	42.0	38.7	2.523	97.6	35.0	2.78	5.99	174.3
6.32	42.0	37.1	2.221	82.4	33.7	2.98	6.18	165.3
6.20	40.3	35.6	2.560	91.1	39.7	3.06	6.05	161.6
6.14	41.6	37.6	2.300	86.5	32.5	2.70	5.85	171.5
7.13	46.5	44.2	2.882	127.4	35.4	2.56	6.34	201.6
8.02	53.1	52.0	3.438	178.8	37.0	2.18	6.67	237.9
9.01	59.7	56.4	3.566	201.1	36.0	1.96	6.58	255.2
10.01	60.8	59.7	3.606	215.3	37.1	1.96	6.96	273.1

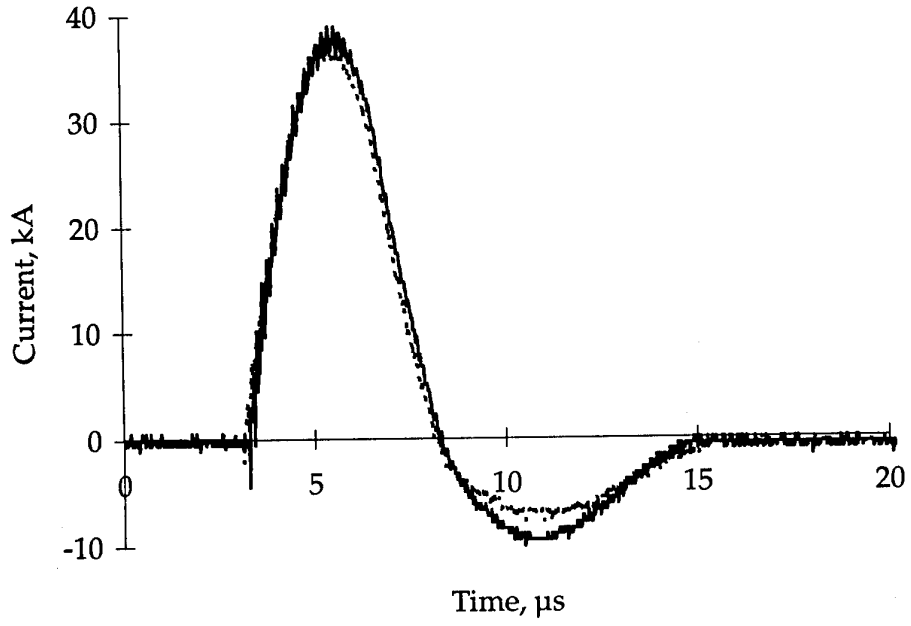

Figure 10: *Current-time histories for two shots at a charge voltage of 5.29 kV.*

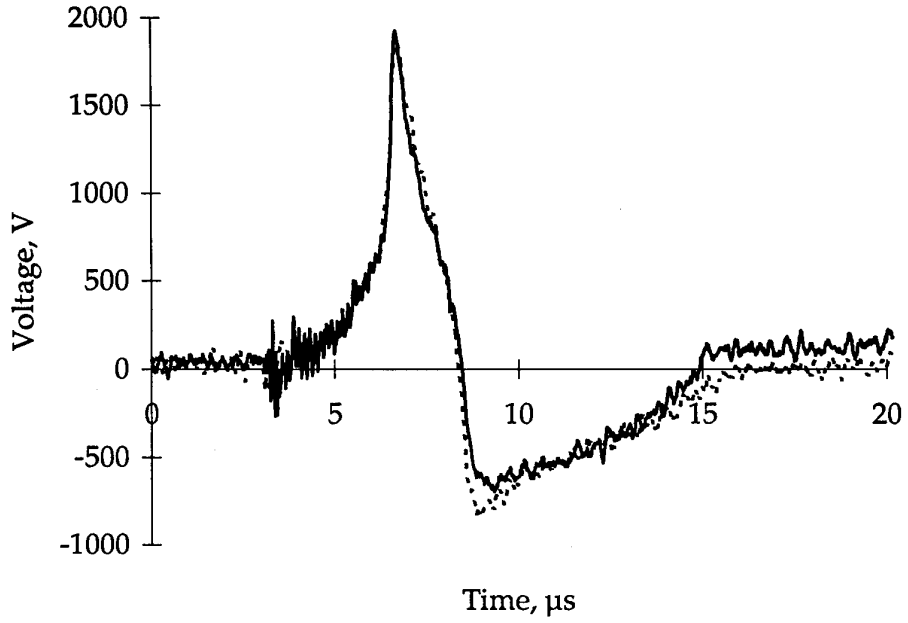

Figure 11: *Bridge foil voltage-time histories for two shots at a charge voltage of 5.29 kV.*

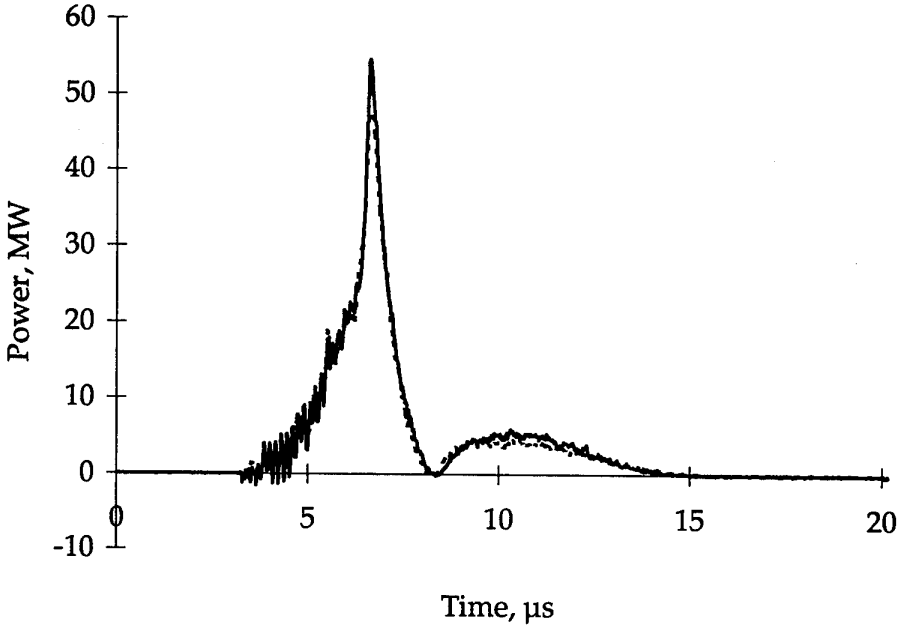

Figure 12: *Power-time histories for two shots at a charge voltage of 5.29 kV.*

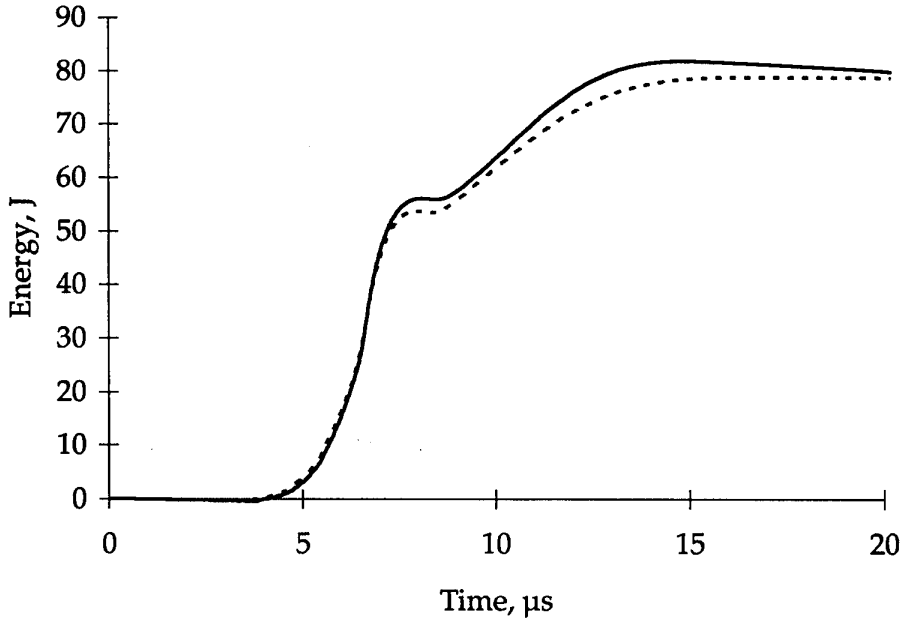

Figure 13: *Energy-time histories for two shots at a charge voltage of 5.29 kV.*

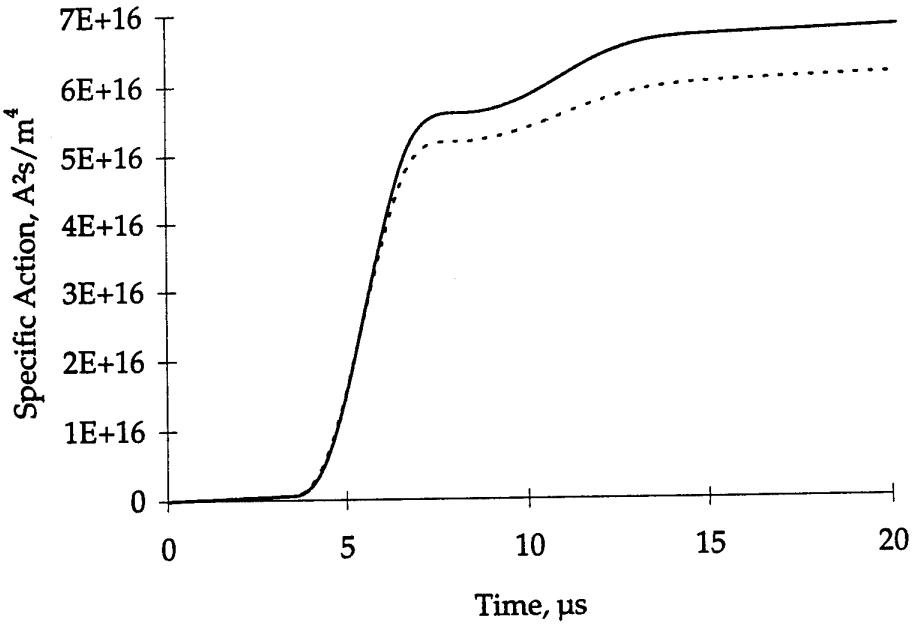

Figure 14: *Specific action-time histories for two shots at a charge voltage of 5.29 kV.*

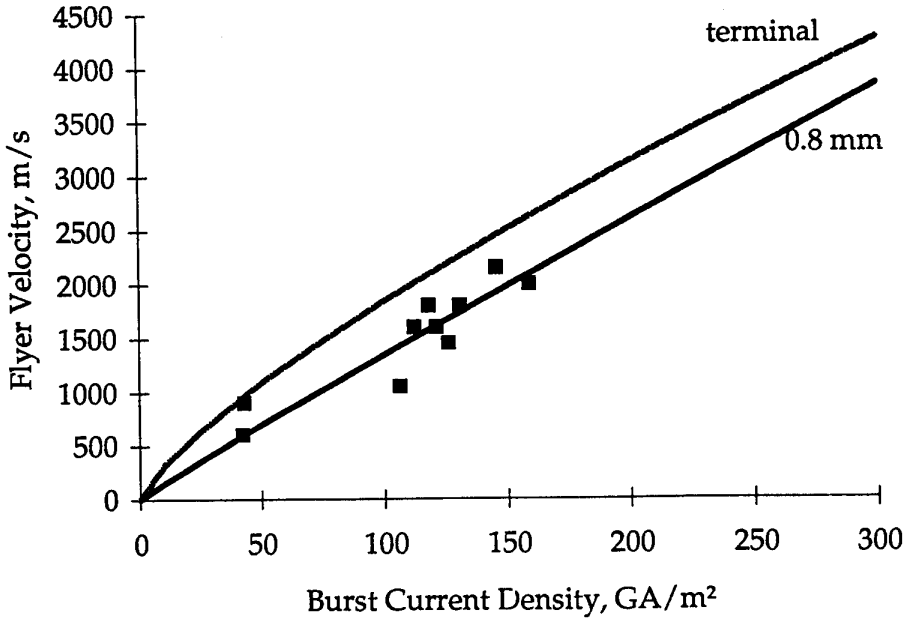

Figure 15: *Flyer velocity versus burst current density experimental data and calculated curves for terminal flyer velocity and flyer velocity at 0.8 mm.*

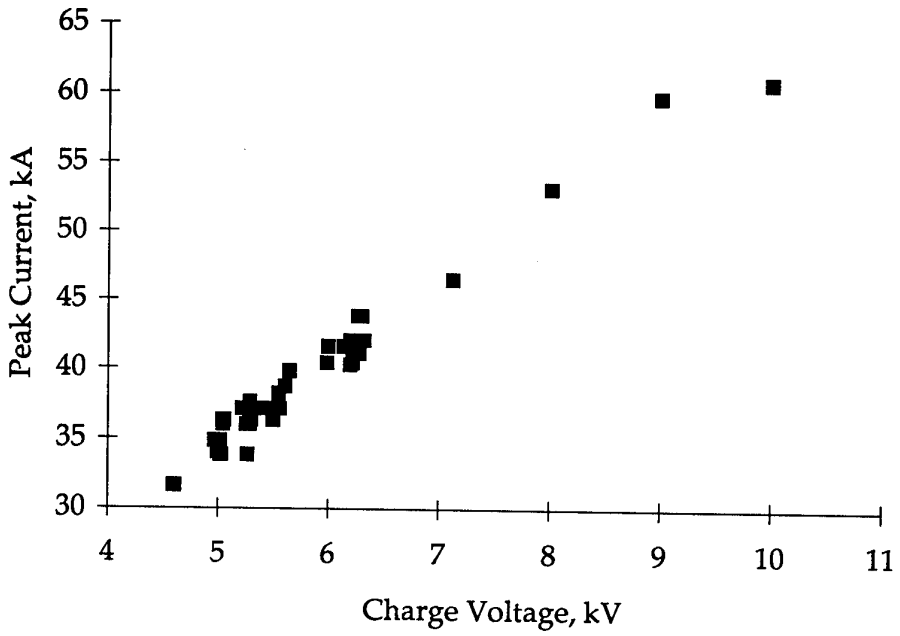

Figure 16: *Peak current versus charge voltage.*

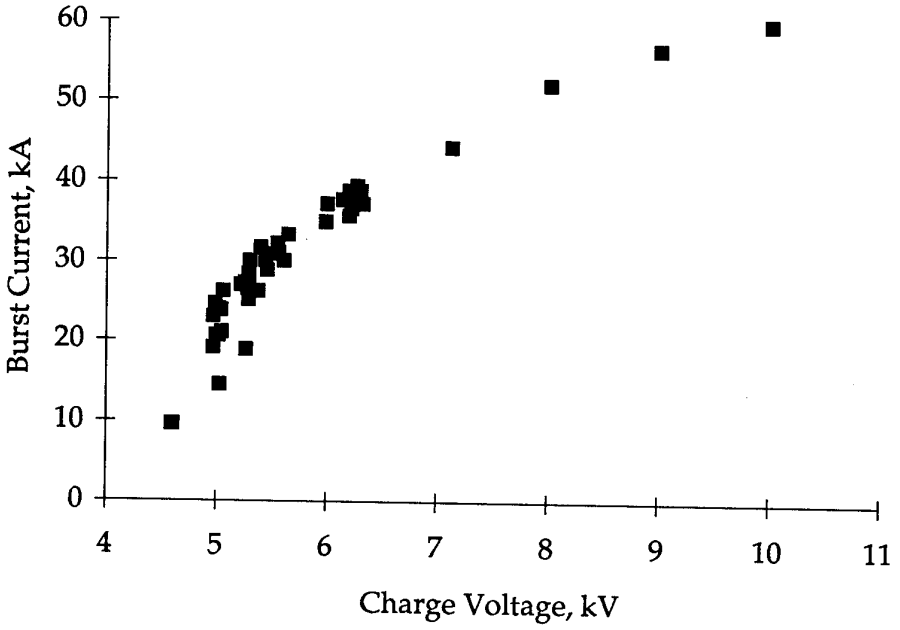

Figure 17: *Burst current versus charge voltage.*

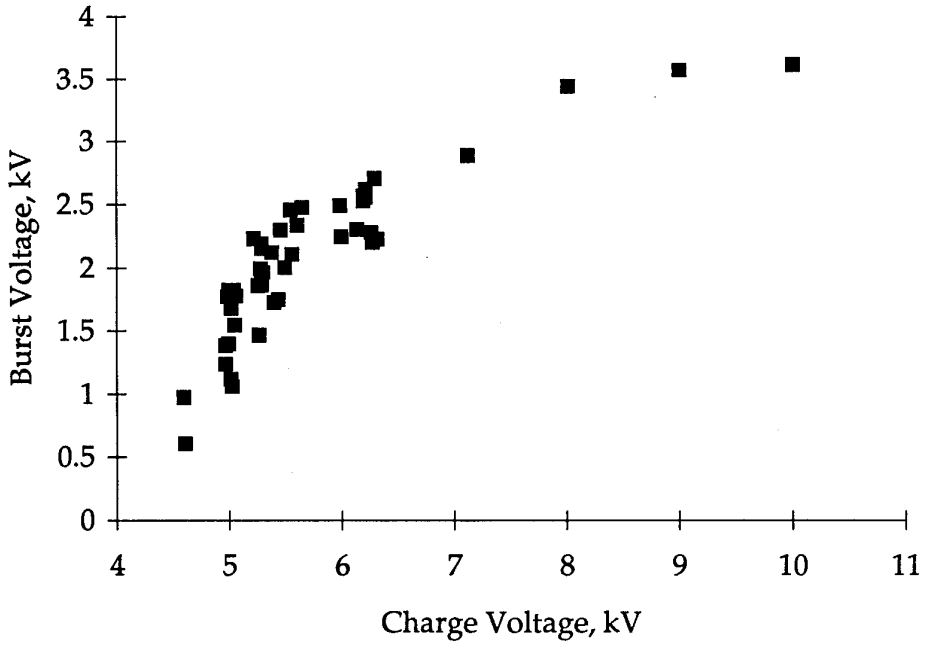

Figure 18: Burst voltage versus charge voltage.

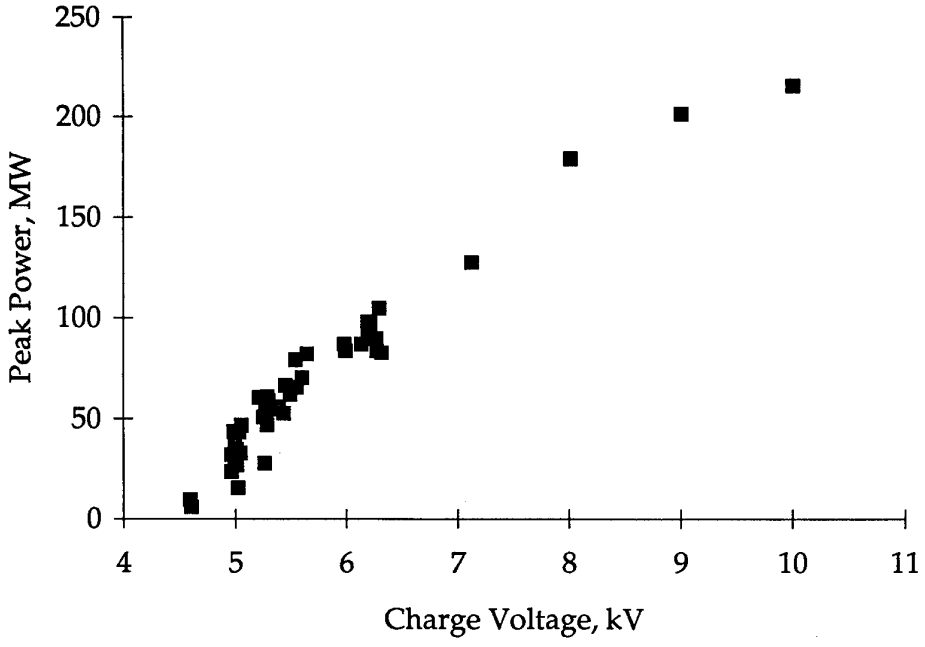

Figure 19: Peak power versus charge voltage.

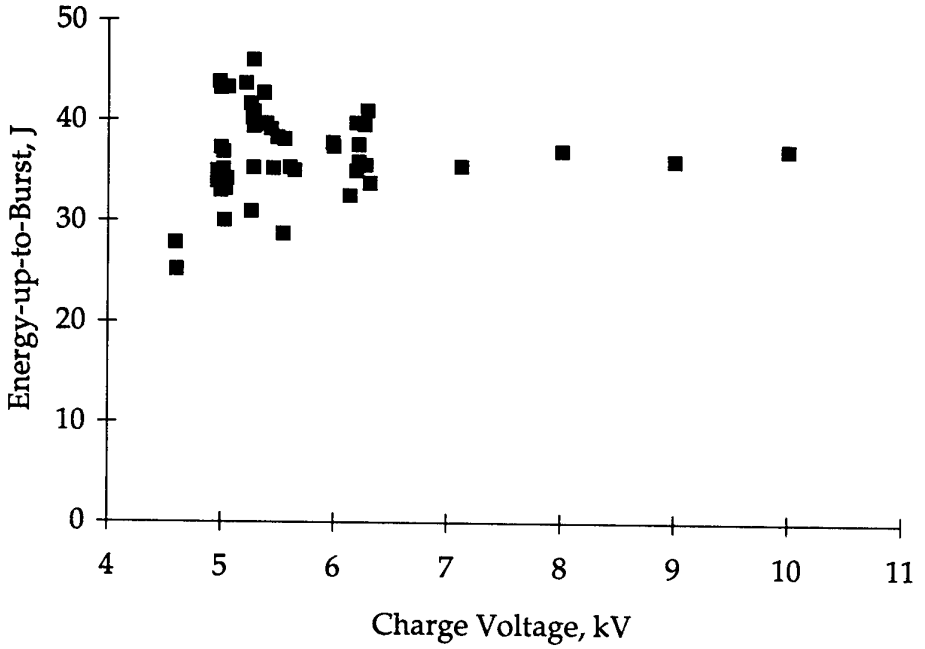

Figure 20: *Energy-deposited-up-to-burst versus charge voltage.*

From ringdowns, the first current peak was found to occur at about 2.7 μs. As shown in Figure 21, $t_b > 2.7$ μs for low V_c and $t_b < 2.7$ μs at high V_c.

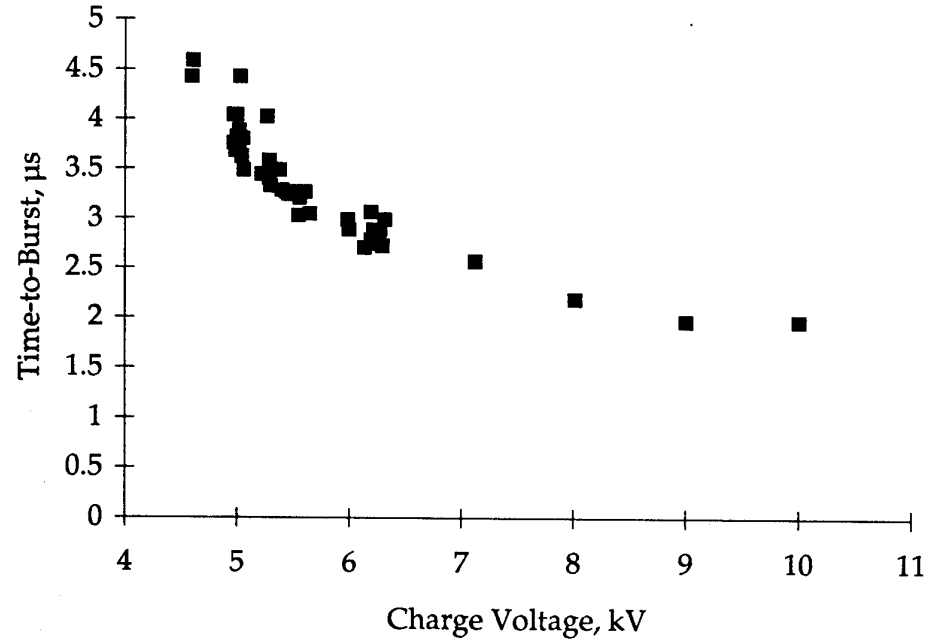

Figure 21: *Time-to-burst versus charge voltage.*

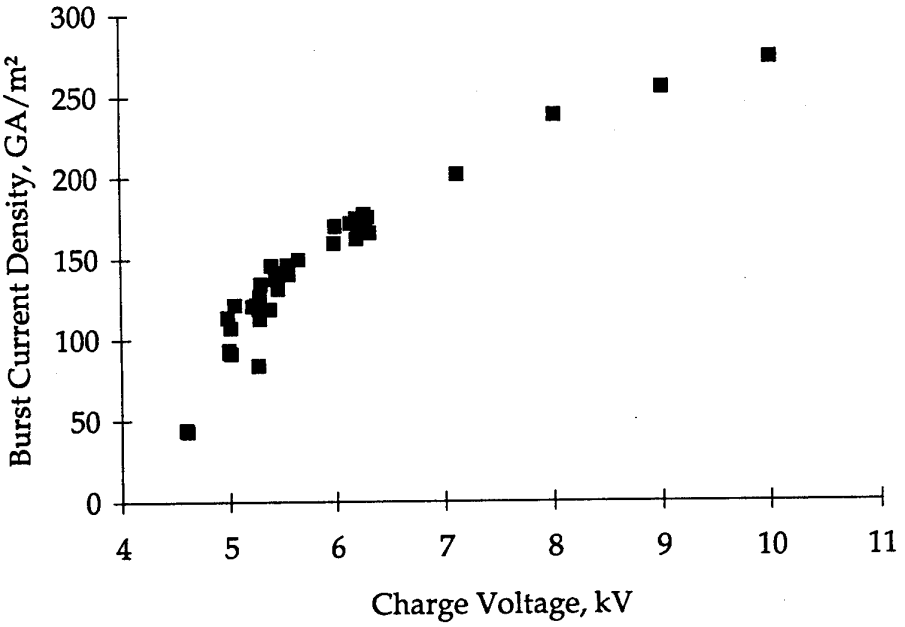

Figure 22: Burst current density versus charge voltage.

5.2 Sensitivity Tests

The results of the sensitivity tests for the two series of PETN, Composition B, and RDX Grade A, Class 1 (recrystallised) are shown in Table 4. For comparison, USA data [4] for these explosives and TNT are also shown in Table 4.

As expected, the two sets of sensitivity data rank the relative shock sensitivity of the explosives in the same order. The AMRL mean charge voltages are consistently higher than the voltages measured by Voreck and Velicky [4]. The disagreement between the mean charge voltages for the two sets increases with decreasing shock sensitivity.

Comparison of flyer velocities at the mean charge voltages can be made using the USA calibration curve, $u_f = 0.4125V_c + 0.7208$ [6] (V_c max = 7.0 kV) and the AMRL calibration curve, $u_f = 1.049V_c - 4.054$ (V_c max = 6.0 kV) and the fitted curve, $u_f = 0.945\sqrt{2}\times1.54\times10^{-4}\ J_b^{\,1.91}$. An estimate of J_b for a given V_C can be obtained from Table 3.

For PETN, u_f =2.44 km/s, 1.58 km/s, and 1.80 km/s, respectively (Table 5). Data reported by Weingart *et al.* [3] suggests the flyer velocity at the initiation threshold is about 1.5 km/s for PETN samples of 25.4 mm diameter pressed from PETN powder with specific surface area of 6000 cm^2/g to density 1.65 Mg/m^3 impacted by a 50 μm

thick Mylar flyer (35.5 mm diameter). They also found that lower density PETN samples were more sensitive, and that initiation or failure must occur close to the impact surface as rarefactions from the rear of the flyer quickly overtake and attenuate the shock front. Particle size and specific surface area for the PETN samples tested by Voreck and Velicky [4] were not reported. Neither were measured for the PETN samples tested in this work. Without knowledge of these parameters, comparisons need to be conservative. However, the flyer velocities are in general agreement.

Table 4: *Comparison of FSTA Sensitivity Data.*

Explosive	Formulation	Density (±σ) (Mg/m^3)	Mean Charge Voltage (±σ) (kV) AMRL	USA [4]
PETN	Pentaerythritol tetranitrate	1.6(±0.05)	5.487(±0.082)	
		1.6(±0.05)	5.260(±0.043)	
		1.67		4.175(±0.062)
RDX (Grade A, Class 1, pressed)	cyclotrimethylenetrinitramine	1.65(±0.05)	6.100(±0.390)	
RDX (Class A)		1.65		4.804(±0.133)
Comp B (pressed)	60%RDX/40%TNT/no wax	1.59(±0.05)	12.43(±0.73)	
	60%RDX/39%TNT/1%Wax	1.59		5.700(±0.136)
TNT (pressed)	Trinitrotoluene	1.49(±0.05)	>14 kV	
		1.36		10.750(±0.760)

For RDX, u_f =2.70 km/s, 2.34 km/s, and 2.24 km/s, respectively. Again the velocities are similar and there has been about the same corresponding incremental increase in charge voltage with respect to the PETN data. As before, the comparisons must necessarily be conservative because of particle size effects and differences in the formulations (e.g., the USA RDX typically contains a small percentage of HMX).

For Composition B, the AMRL mean charge voltage is greater than the calibration curve range. The flyer velocities are thus u_f =3.07 km/s (USA) and u_f =3.85 km/s (AMRL fitted curve). The flyer velocities are similar even though the mean charge voltages are markedly different.

Table 5: *Comparison of Flyer Velocities.*

Explosive	Flyer Velocity (km/s) USA Calibration Curve	AMRL Calibration Curve	AMRL Fitted Curve
PETN	2.44	1.58	1.80
RDX	2.70	2.34	2.24
Comp B	3.07	-	3.85

Flyer velocity as a function of charge voltage is linear over the range 4.0-7.0 kV for the USA tester. The mean charge voltages for PETN, RDX, and Composition B given by this tester fall in this range. However, for the AMRL tester collectively the explosive tests, the fitted curve, and I_b suggest the relationship for the charge voltages above 6 kV is non-linear. Only the mean charge voltages for PETN and RDX occur in the linear range.

In the above analysis it has been assumed that the AMRL fitted curve is a valid one. Confirmation of this awaits a further calibration using a modified VISAR as mentioned in Section 5.1.

The test interval for the Bruceton analysis was arbitarily chosen to be 200 volts. By the end of the explosive tests it was considered that this interval would in general be an appropriate one, particularly for sensitive explosives (e.g., PETN).

The difficulty in go/no-go discrimination that is likely to occur for some of the less sensitive explosives is of some concern, particularly in the event the FSTA is used by less knowledgeable and experienced operators. The range of typical witness plate damage is shown in Figure 23. The damage sustained by the middle example represents the case where lateral expansion of the holder also needs to be considered when assigning a go or no-go to the event. At least 30 tests were performed for each explosive tested in this work. It is considered that at least this number of tests should be used when discrimination is an issue.

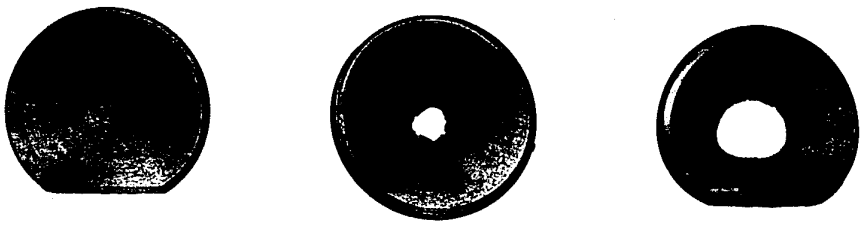

Figure 23: Typical damage to witness plates.

6. Conclusions

The AMRL flyer sensitivity test apparatus uses flyer plates accelerated by the electric gun technique. It is a research tool that was constructed for studying particle size effects on the shock sensitivity of explosives initiated by short duration shocks. The charge voltage versus flyer velocity calibration was performed over a voltage range of 4.6-6 kV while a comprehensive electrical characterization was performed over a charge voltage range of 4.6-10 kV. Calibration and explosive tests for PETN, RDX, and Composition B together have shown that the performance of the AMRL FSTA is different from the USA test apparatus which it was meant to replicate; the difference was attributed to different electrical characteristics. The AMRL FSTA was found to be limited to a shock sensitivity range represented by PETN (high shock sensitivity) and Composition B (low shock sensitivity) whereas explosives less sensitive than Composition B, e.g., TNT, are able to be tested on the USA apparatus.

It is envisaged that AMRL particle size effect studies initially would involve RDX formulations with shock sensitivities similar to RDX and thus within the capability of the FSTA. If a requirement arose to match the performance more closely to the USA equipment (e.g., to test explosives less sensitive than Composition B) this would require the use of an alternative capacitor and perhaps a thinner bridge foil. As the charge voltage for the calibration using a VISAR velocity interferometer was limited to 6 kV, due to electrical noise problems, it is proposed that a future calibration to 10 kV be performed using a fibre-optic conversion of the VISAR.

7. Acknowledgements

Dr Don Richardson was responsible for the initial specification and construction phase of the FSTA with assistance from Brian Jones. Ken Lee and Mark Cleeland subsequently provided assistance with modifying its electrical circuitry. Mark Cleeland also prepared many of the stripline assemblies. Mark Fitzgerald assisted with the calibration of the FSTA.

8. References

1. Spear, R. J. and Nanut, V. (1987).
Mechanism of and Particle Size Effects on Shock Sensitivity of Heterogeneous Pressed Explosives: Preliminary Assessment of Binderless RDX in Fuze Trains.
(MRL Report MRL-R-1077). Maribyrnong, Vic.: Materials Research Laboratory.

2. Wolfson, M. G. (1983).
The MRL Small Scale Gap Test for the Assessment of Shock Sensitivity of High Explosives.
(MRL Report MRL-R-896). Maribyrnong, Vic.: Materials Research Laboratory.

3. Weingart, R. C., Lee, R. S., Jackson, R. K., and Parker, N. L. (1976)
Acceleration of thin flyers by exploding metal foils: application to initiation studies.
In: *Proceedings of the Sixth Symposium (International) on Detonation.*

4. Voreck, W. E. and Velicky, R. W. (1981)
Exploding Foil Shock Sensitivity Test. In:*Proceedings of the Seventh Symposium (International) on Detonation.*

5. Velicky, R. W. (1986)
An explosive output laboratory test employing the slapper technique to stimulate detonations. Technical Report ARAED-TR-86036. Limited Distribution. Dover, New Jersey: US Army Armament Research, Development and Engineering Center.

6. Voreck, W. E. (1983).
_____. Seventh Explosive Device Technology Exchange Group Meeting.

7. Hatt, D. J. (1991)
A VISAR Velocity Interferometer System at MRL for Slapper Detonator and Shockwave Studies. (MRL Technical Report MRL-TR-91-42). Maribyrnong, Vic.: Materials Research Laboratory.

8. MRL Design Drawing MRL-3469 (1988)

9. Podlesak, M. (1990)
Rogowski Coil Calibration on a Capacitive Discharge Rig without the use of a Current Reference. Review of Scientific Instruments, 61(2)

10. Podlesak, M., Richardson, D. D., and Olsson, C. (1993)
An Exploding Foil Flying Plate Generator for Shock Wave Studies - Calibrations. (MRL Research Report MRL-RR-1-92). Maribyrnong, Vic.: Materials Research Laboratory.

11. Hatt, D. J. and Ryan, P. F. X. (1993)
Calibration and Testing of a Large-Scale Electric Gun for Shock Hugoniot Measurement. (MRL Technical Report MRL-TR-93-24). Maribyrnong, Vic.: Materials Research Laboratory.

12. Hatt, D. J. and Waschl, J. W. (1991)
Performance Evaluation of an EBF Generated Thin Flyer Plate. (MRL Technical Report MRL-TR-91-28). Maribyrnong, Vic.: Materials Research Laboratory.

13. Anderson, G. W. and Neilson, F. W. (1959)
Use of the "Action Integral" in Exploding Wire Studies. In: *Exploding Wires Vol. 1. (Eds) W. G. Chace and H. K. Moore.* New York, Plenum Press.

14. Lee, R. S. (1986)
An Analytical Model for the Dynamic Resistivity of Electrically-Exploded Conductors. In: *Proceedings of the Thirteenth Symposium on Explosives and Pyrotechnics.*

15. _____. (1988)
Asystant GPIB. Asyst Software Technologies, Inc. NY, USA.

16. Culling, H.P. (1953)
Statistical methods appropriate for evaluation fof fuze explosive-train safety and reliability. (NAVORD Report 2101) . US Naval Ordnance Laboratory, Whiteoak, MD.

17. Chau, H. H., Dittbenner, G., Hofer, W. W., Honedel, C. A., Steinberg, D. J., Stroud, J. R., Weingart, R. C., and Lee, R. S. (1980).
Electric gun: a versatile tool for high-pressure shock-wave research.
Rev. Sci. Instrum. **51** (12).

This page intentionally left blank

Appendix A

Instructions for the preparation of stripline assemblies

1. Using large (25 cm) scissors, cut two sheets from 0.13 mm thick copper foil to the dimensions shown in Figure A1. Measurements can be made with a steel rule.

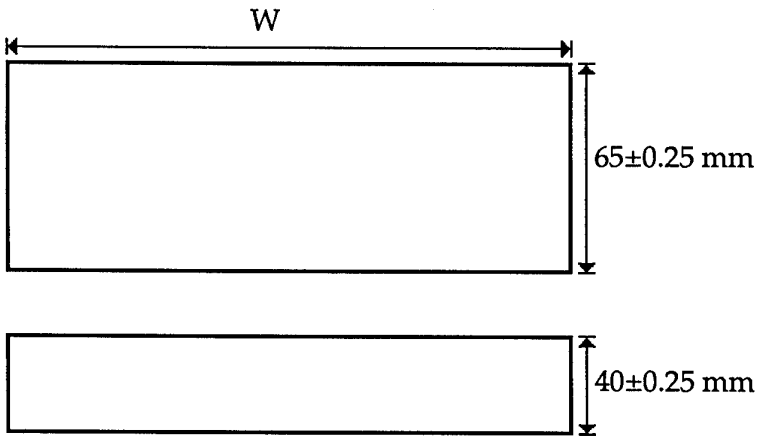

Figure A1: Dimensions for copper foil sheets. W = width as supplied (≈ 150 mm).

2. Using a precision rotary cutter, cut a 0.125 mm thick Mylar strip to the dimensions shown in Figure A2. Width of the strip can be measured with an engineer's microscope.

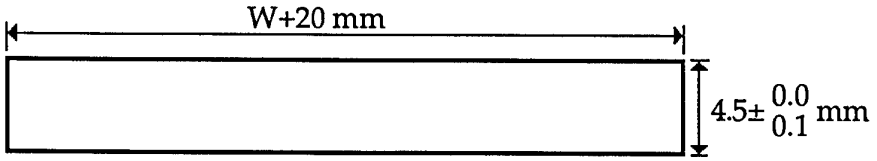

Figure A2: Dimensions for Mylar strip.

3. Using masking tape, affix the large copper sheet to a plate glass work-top (Fig. A3).

4. Using a brass bar (200 mm x 20 mm x 4.5 mm) as a spacer, affix the smaller copper sheet to the glass work-top (Fig. A3).

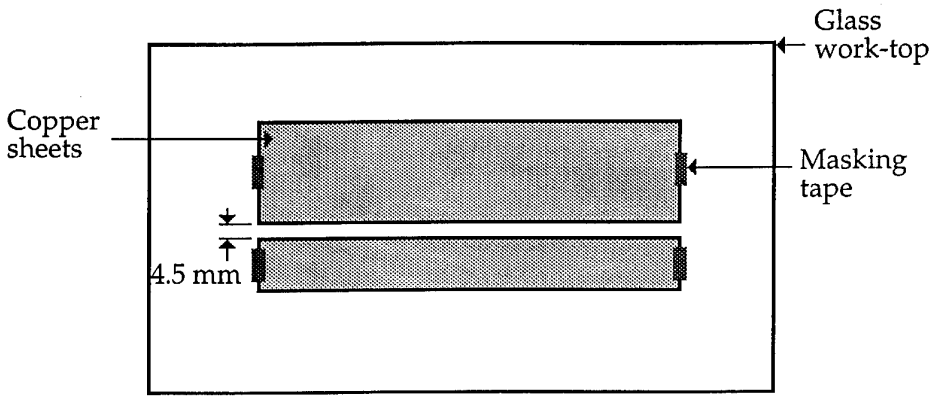

Figure A3: Layout of copper sheets on glass work-top.

5. Remove the brass bar and lay 19 mm wide polyester tape across the space between the copper sheets.

6. Remove the assembly from the work-top and trim off excess polyester tape.

7. Return the assembly to the work-top but with the adhesive side of the polyester tape facing upwards. Place the 4.5 mm wide Mylar strip in the space between the copper sheets and press down firmly onto the adhesive tape.

8. Remove the assembly from the work-top and trim Mylar strip flush to copper sheets (Fig.A4a).

9. Using the large scissors, cut the assembly into 12.5 ±0.25 mm wide strips (Fig. A4b).

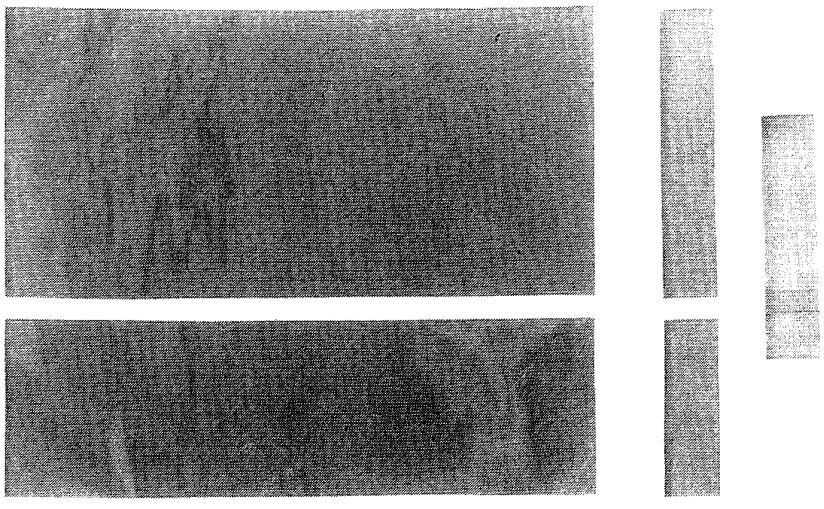

Figure A4: Photographs of copper sheets and Mylar strip before and after cutting and folding.

10. To fold the strips, place each strip on the work-top and mark with pencil at the fold line shown in Figure A5a. Align a 150 mm steel rule with the mark and hold down with finger pressure. Slide another steel rule under the strip and bend the strip until it is normal to the glass surface. Complete the fold with the fingers (Fig. A4c).

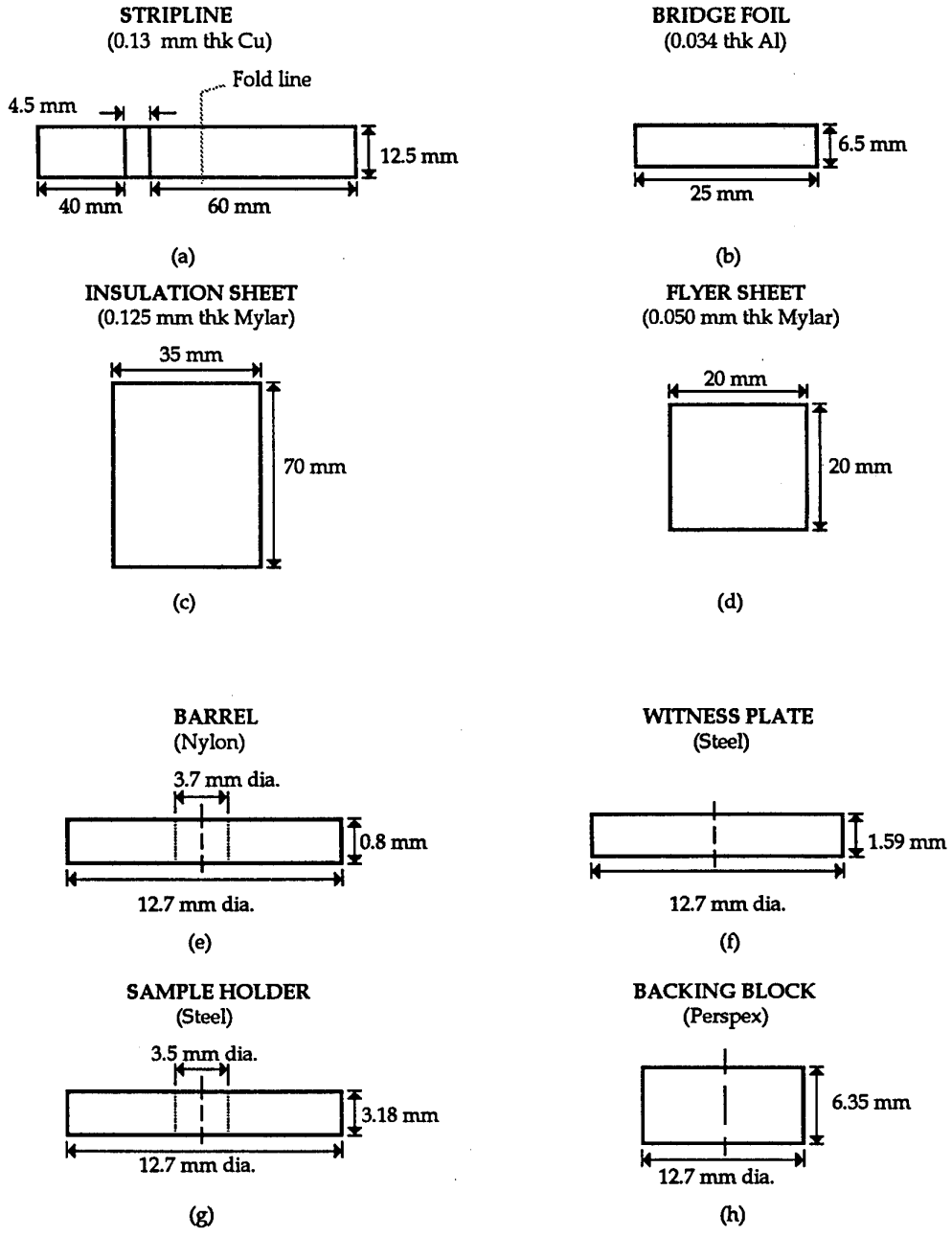

Figure A5: Components employed in the manufacture of the stripline assemblies.

11. Using the rotary cutter, cut a 6.5±0.1 mm wide strip from 0.034 mm thick aluminium foil sheet. Remove wrinkled edge of the strip by covering the strip with a sheet of paper and stroking paper with a flat metal plate. Bridge foils (Fig. 5Ab)are obtained by cutting the strip into 25±0.5 mm lengths.

12. Using the rotary cutter, cut Mylar insulation and flyer sheets to the dimensions shown in Figures A5 c and d.

13. Insert an insulation sheet between a copper stripline. Position a bridge foil centrally over the gap in the stripline and affix to the stripline with 12 mm wide "magic" tape (Fig. A6).

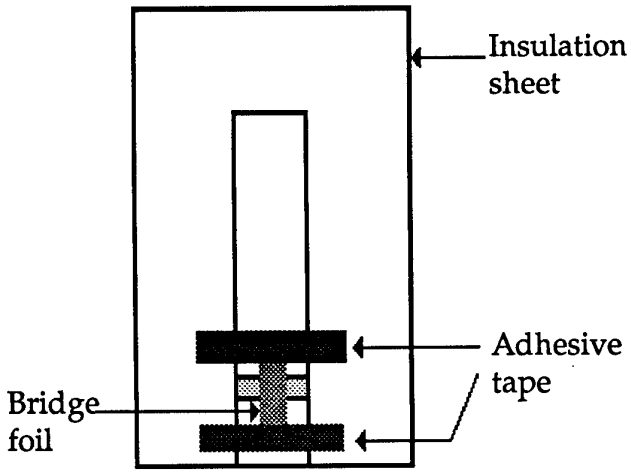

Figure A6: Placement of insulation sheet and bridge foil. Position tape as close as possible to the gap in copper stripline without the tape being in the barrel footprint (this is to ensure that close contact can be obtained between the tamper, bridge foil and flyer sheet).

14. Tape a flyer sheet over the bridge foil; tape one end only as shown in Figure A7.

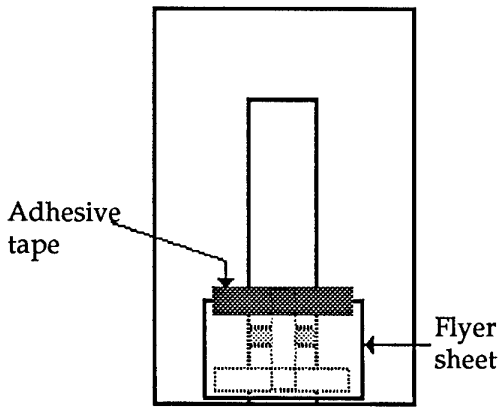

Figure A7: Placement of flyer sheet.

15. Position barrel centrally (by eye) over the gap and scribe an alignment arc with a felt tipped pen. Scribe at least a half circle. Affix a Nylon barrel (Fig. A5e) to the flyer sheet with a few drops of cyanoacrylate adhesive (make sure adhesive isn't extruded into the barrel opening).

16. Affix a witness disc (Fig. A5f) to a filled explosive sample holder (Fig. 5Ag) with cyanoacrylate adhesive.

17. Simultaneously hold with the fingers the explosive holder and witness disc on the barrel and the Perpex backing block (Fig. A5h) underneath the barrel against the stripline. Clamp in place with a bent paper clip (Fig. A8) and then align all components by eye to the barrel.

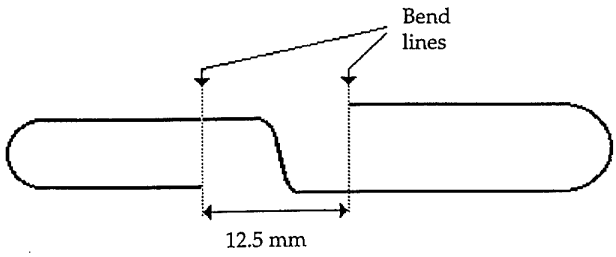

(a)

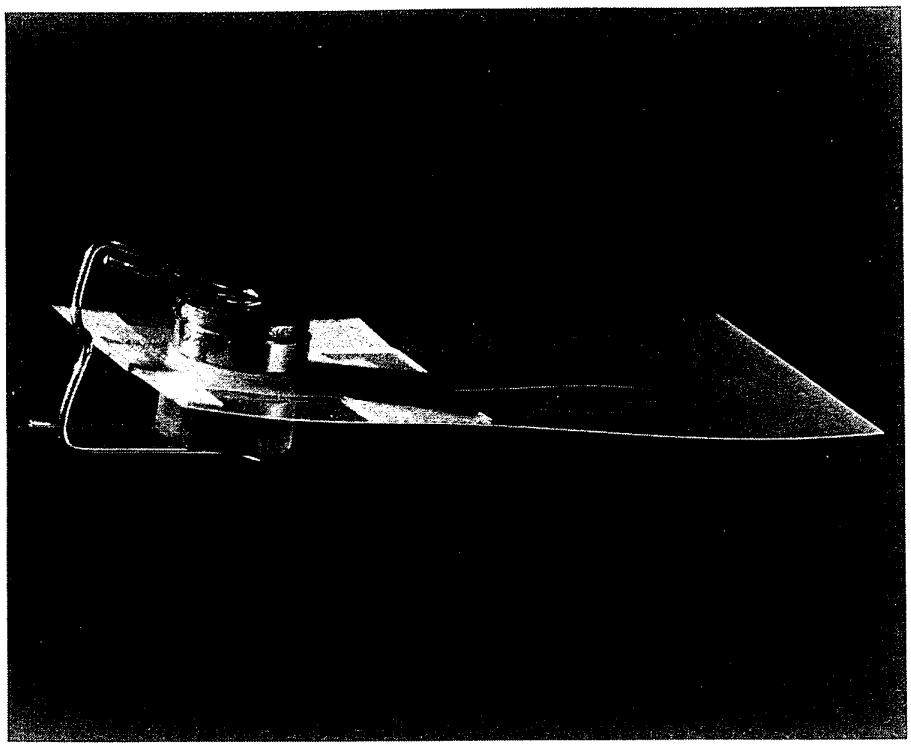

(b)

Figure A8: *Paper clip clamp: (a) Unfolded clip and position of 100°-110° bends. A 12.5 mm square brass bar is employed as a width gauge. If the clip loops are not coplanar after bending, adjustments are made with pliers; (b) Photograph of a completed assembly.*

Construction, Characterization and Evaluation of the AMRL
Flyer Sensitivity Test Apparatus

David J. Hatt and Michael G. Wolfson

(DSTO-TR-0218)

DISTRIBUTION LIST

DEFENCE ORGANISATION

Defence Science and Technology Organisation

Chief Defence Scientist
FAS Science Policy
AS Science Corporate Management
} shared copy
Counsellor Defence Science, London (Doc Data Sheet only)
Counsellor Defence Science, Washington (Doc Data Sheet only)
Scientific Adviser to Thailand MRD (Doc Data Sheet Only)
Scientific Adviser to the DRC (Kuala Lumpur) (Doc Data Sheet Only)
Senior Defence Scientific Adviser/Scientific Adviser Policy and Command (shared copy)
Navy Scientific Adviser (3 copies Doc Data Sheet)
Scientific Adviser - Army (Doc Data Sheet only)
Air Force Scientific Adviser
Director Trials

Aeronautical and Maritime Research Laboratory

Director
Chief, Weapons Systems Division
Dr R.J. Spear
Dr D.D. Richardson
Mr D.J. Hatt
Mr M.G. Wolfson

DSTO Library

Library Fishermens Bend
Library Maribyrnong
Main Library DSTOS (2 copies)
Library, MOD, Pyrmont (Doc Data sheet only)

Defence Central

OIC TRS, Defence Central Library
Officer in Charge, Document Exchange Centre, 1 copy
DEC requires, as permitted by the release limitations, the following copies to meet exchange agreements under their management:
*US Defence Technical Information Centre, 2 copies
*UK Defence Research Information Centre, 2 copies
*Canada Defence Scientific Information Service, 1 copy
*NZ Defence Information Centre, 1 copy
National Library of Australia, 1 copy
The Director, Qinghua University, Beijing, 1 copy
The Librarian, Beijing University of Aeronautics, 1 copy
The Librarian, Institute of Mechanics, Chinese Academy of Sciences, 1 copy
Defence Intelligence Organisation
Library, Defence Signals Directorate (Doc Data Sheet only)

DISTRIBUTION LIST
(Continued)

(DSTO-TR-0218)

Army

Director General Force Development (Land) (Doc Data Sheet only)
ABCA Office, G-1-34, Russell Offices, Canberra (4 copies)
NAPOC QWG Engineer NBCD c/- DENGRS-A, HQ Engineer Centre

Navy

ASSTASS, APW2-1-OA2, Anzac Park West, Canberra (Doc Data Sheet only)

UNIVERSITIES AND COLLEGES

Australian Defence Force Academy
Library
Head of Aerospace and Mechanical Engineering
Deakin University, Serials Section (M list)), Deakin University Library, Geelong, 3217,
Senior Librarian, Hargrave Library, Monash University

OTHER ORGANISATIONS

NASA (Canberra)
AGPS

ABSTRACTING AND INFORMATION ORGANISATIONS

INSPEC: Acquisitions Section Institution of Electrical Engineers
Library, Chemical Abstracts Reference Service
Engineering Societies Library, US
American Society for Metals
Documents Librarian, The Center for Research Libraries, US

INFORMATION EXCHANGE AGREEMENT PARTNERS

Acquisitions Unit, Science Reference and Information Service, UK
Library - Exchange Desk, National Institute of Standards and
Technology, US

DEFENCE SCIENCE AND TECHNOLOGY ORGANISATION DOCUMENT CONTROL DATA	1. PAGE CLASSIFICATION UNCLASSIFIED 2. PRIVACY MARKING/CAVEAT (OF DOCUMENT)

3. TITLE	4. SECURITY CLASSIFICATION (FOR UNCLASSIFIED REPORTS THAT ARE LIMITED RELEASE USE (L) NEXT TO DOCUMENT CLASSIFICATION)
Construction, characterization and evaluation of the AMRL flyer sensitivity test apparatus	Document (U) Title (U) Abstract (U)
5. AUTHOR(S) David J. Hatt and Michael G. Wolfson	6. CORPORATE AUTHOR Aeronautical and Maritime Research Laboratory PO Box 4331 Melbourne Vic 3001

7a. DSTO NUMBER	7b. AR NUMBER	7c. TYPE OF REPORT	8. DOCUMENT DATE
DSTO-TR-0218	AR-009-347	Technical Report	November 1995

9. FILE NUMBER	10. TASK NUMBER	11. TASK SPONSOR	12. NO. OF PAGES	13. NO. OF REFERENCES
510/207/0289	DST 94/228		44	17

14. DOWNGRADING/DELIMITING INSTRUCTIONS	15. RELEASE AUTHORITY
	Chief, Weapons Systems Division

16. SECONDARY RELEASE STATEMENT OF THIS DOCUMENT

Approved for public release

OVERSEAS ENQUIRIES OUTSIDE STATED LIMITATIONS SHOULD BE REFERRED THROUGH DOCUMENT EXCHANGE CENTRE, DIS NETWORK OFFICE, DEPT OF DEFENCE, CAMPBELL PARK OFFICES, CANBERRA ACT 2600

17. DELIBERATE ANNOUNCEMENT

Announcement of this report is unlimited

18. CASUAL ANNOUNCEMENT YES/NO (Cross out whichever is not applicable)

19. DEFTEST DESCRIPTORS

Propellant sensitivity; Explosives; Particle size; Electric gun; Velocity measurement; Interferometers; TNT; Composition B explosive; RDX

20. ABSTRACT

The AMRL flyer sensitivity test apparatus (FSTA) uses the electric gun technique to accelerate 50 μm thick plastic flyer plates of about 3.5 mm in diameter to high velocity. Impacting high explosives with the flyer plates generates short duration shock pulses with sufficient energy to cause ignition. By varying the charge voltage, and hence the flyer velocity, the relative shock sensitivity of explosives can be measured. Detonation or non-detonation of the explosive is indicated by the level of damage to a steel witness plate. The FSTA was found to be suitable for testing 50 mg samples of pressed explosives with shock sensitivities in the range represented by PETN (high) to Composition B (low). A flyer velocity versus charge voltage calibration up to a charge voltage of 6 kV was performed using a VISAR velocity interferometer. The shock sensitivity can be related to charge voltage in the range 5-10 kV or flyer velocity in the range 2-4 km/s. A comparison of the FSTA with similar USA testers is presented.